

REVIEW

View Article Online
View Journal | View Issue



Cite this: *Mater. Horiz.*, 2024, **11**, 2772

Intelligent micro/nanorobots based on biotemplates

Ting Chen,^a Yuepeng Cai,^b Biye Ren,^{ib} ^{*a} Beatriz Jurado Sánchez ^{ib} ^{*c} and Renfeng Dong ^{ib} ^{*bd}

Intelligent micro/nanorobots based on natural materials as biotemplates are considered to be some of the most promising robots in the future in the microscopic field. Due to the advantages of biotemplates such as unique structure, abundant resources, environmental friendliness, easy removal, low price, easy access, and renewability, intelligent micro/nanorobots based on biotemplates can be endowed with both excellent biomaterial activity and unique structural morphology through biotemplates themselves and specific functions through artificial micro/nanotechnology. Thus, intelligent micro/nanorobots show excellent application potential in various fields from biomedical applications to environmental remediation. In this review, we introduce the advantages of using natural biological materials as biotemplates to build intelligent micro/nanorobots, and then, classify the micro/nanorobots according to different types of biotemplates, systematically detail their preparation strategies and summarize their application prospects. Finally, in order to further advance the development of intelligent micro/nanorobots, we discuss the current challenges and future prospects of biotemplates. Intelligent micro/nanorobots based on biotemplates are a perfect combination of natural biotemplates and micro/nanotechnology, which is an important trend for the future development of micro/nanorobots. We hope this review can provide useful references for developing more intelligent, efficient and safe micro/nanorobots in the future.

Received 31st January 2024,
Accepted 22nd March 2024

DOI: 10.1039/d4mh00114a

rsc.li/materials-horizons

Wider impact

This review aims to be a comprehensive, authoritative, critical, and accessible review of general interest to the scientific community because it covers the recent progress and application of natural biological materials as biotemplates for developing micro/nanorobots, including the common plant tissues, bacteria, cells, and microalgae available in nature. Utilizing natural materials as biotemplates to obtain intelligent micro/nanorobots is a new trend in recent years due to their elegant structures and abundant surface functional groups. To further expand the potential of intelligent micro/nanorobots for applications, several challenges should be urgently considered and addressed. This review will target a broad audience from chemistry, biochemistry to environmental chemistry communities. Main applications covered will be targeted to the chemical/biochemical field, including drug delivery, biological sensing, bacterial inactivation and environmental remediation approaches *via* chemical sorption and degradation. Firstly, the advantages of biotemplates, preparation processes and propulsion modes of micro/nanorobot synthesis using biotemplates with different structures are systematically introduced. Secondly, based on the characteristics of biotemplates, their intelligent applications in environmental chemistry and biomedicine are elaborated. Finally, the current problems and challenges in synthesizing intelligent micro/nanorobots are reviewed, along with future prospects (to stimulate further research in the scientific community).

1. Introduction

With the continuous development of robot technology, robots with different functions play a more critical role in various fields and have become humans right-hand men.¹ However, when the robot operations need to enter from the macro scale to the micro scale, such as intravascular drug transportation and intracellular micro-operation, macro robots should be reduced in size to reach the target location to complete the established tasks.² Thus, it is urgent to develop microrobots or nanorobots that can work at the micro/nano scale, namely

^a School of Materials Science and Engineering, South China University of Technology, Guangzhou 510640, China. E-mail: mcbyren@scut.edu.cn

^b School of Chemistry, South China Normal University, Guangzhou 510006, China. E-mail: rfdong@m.scnu.edu.cn

^c Department of Analytical Chemistry, Physical Chemistry, and Chemical Engineering Universidad de Alcalá, Alcalá de Henares, E-28802 Madrid, Spain. E-mail: beatriz.jurado@uah.es

^d School of Chemistry and Chemical Engineering, Key Laboratory of Clean Energy Materials, Chemistry of Guangdong Higher Education Institutes Lingnan Normal University Zhanjiang, Guangdong 524048, P. R. China



micro/nanorobots. Micro/nanorobots mainly refer to artificial robots that convert energy (such as chemical energy,³ light,⁴ electric energy,⁵ magnetic field,⁶ and ultrasonic wave⁷) from the external environment into their motion.^{8,9} Owing to the

controllable motion behavior and the high efficiency of micro/nanorobots, they displayed significant potential for various applications, such as environmental remediation,¹⁰ biodegradation,¹¹ detection,¹² active drug delivery,¹³ and micro/nanosurgery.¹⁴ Based on the different applications of micro/nanorobots, various preparation methods, shapes, and material sources have emerged.¹⁵ Due to the significant differences in structures and material sources, optimizing the structures and materials of these micro/nanorobots for broader applications is necessary. Despite significant micro/nanorobot fabrication achievements, conventional chemical or artificially synthetic materials emerge with obvious limitations, such as low structural reproducibility, low batch fabrication efficiency and high prices.

The fine structure and easy accessibility of natural organisms have inspired researchers.¹⁶ In order to survive in nature, organisms gradually acquire the ability to adapt to various changes in complex natural environments. They have evolved a large number of dominant structures and biological forms in



Ting Chen

Ting Chen has been a PhD student at the School of Materials Science and Engineering, South China University of Technology (SCUT), since 2020. Her research interests focus on the template preparation of micro/nanorobots for detection and biomedical applications, including hard and soft templates.



Yuepeng Cai

Yuepeng Cai received his PhD degree in 2002 from Sun Yat-Sen University under the supervision of Prof. Bei-Sheng Kang. He became a professor of chemistry at South China Normal University (SCNU) in 2004 and has served as the dean of the School of Chemistry at SCNU in 2019. His current research interests focus on the synthesis of nanomaterials and their applications in energy conversion and storage.



Biye Ren

Biye Ren obtained his PhD degree from South China University of Technology (SCUT), China in July 1999. He is now a full professor and doctoral supervisor at the School of Materials Science and Engineering, South China University of Technology, China. His research interests focus on controllable polymer self-assembly, resin synthesis and application, and the application of micro/nanorobots.



Beatriz Jurado Sánchez

Beatriz Jurado Sánchez has been an Associate Professor at the University of Alcalá (Madrid, Spain) since 2022. From 2017 to 2022 she was a Ramón y Cajal researcher at the same University. She received her PhD in chemistry from the University of Cordoba in 2009. In 2013 she was awarded the prestigious Marie Curie IOF fellowship. Prof. Jurado has co-authored over 89 scientific papers (H Index = 38), 5 book chapters and more than 20 communications in international conferences. Her current research interests focus on self-propelled micromotors for analytical and biomedical applications. She is currently an Associate Editor for RSC Advances and an Early Advisory Board Member of Analytical Chemistry.

on nanomotors, functional micro/nanomaterials, self-propelled nanosystems.



Renfeng Dong

Renfeng Dong is currently an associate professor at School of Chemistry, South China Normal University (SCNU). He obtained his PhD degree in Materials Science from South China University of Technology (SCUT) in 2016. He has been a joint PhD student in the University of California, San Diego (UCSD) from 2012–2014 and a CSC fellow. He was a postdoctoral fellow at SCNU from 2016–2018. His current research interests focus

on nanomotors, functional micro/nanomaterials, self-propelled nanosystems.



the process of continuous evolution and can accurately control these morphological structures at the micro or nano scale through their regulatory mechanism.¹⁷ From the natural calcified biotube crystals, hollow fibers, helix vessels, and spiny protrusion pollen to magnetostatic bacteria and nature cells, biotemplates can generate various highly ordered hierarchical structures and unique biological activities on different size scales. At the micro and nanometer scales, their structures often have an advanced level of intricacy that rivals the sophistication of current engineered materials and systems.¹⁸ In addition, the surface of biotemplates is rich in active functional groups that can be used directly for synthesis, avoiding the tedious chemical synthesis process.¹⁹ Therefore, in recent years, many researchers have achieved through biotemplates the morphological and functional diversification of synthetic materials that meet the environmental protection requirements for materials. Biotemplates can effectively transform highly structured natural structures into multifunctional materials through artificial modification, such as using plant fibers, microalgae, cell membranes, and bacteria to prepare functional materials with diverse shapes and functions.¹⁵ In addition, using biotemplates as raw materials has many advantages, such as unique configuration, high morphological repeatability, abundant resources, environmental friendliness, easy removal, cheap, easy availability, and renewability.^{20,21} It is a new method and way to obtain micro/nanorobots with special structures.²² Natural biotemplates with inherent good biocompatibility and a delicate structure provide new opportunities for preparing multifunctional micro/nanorobots.²³

Using the natural structure of biotemplates solves the challenging problems encountered in research to a certain extent. Integrating biotemplates and micro/nanotechnology not only retains the biological activity of biotemplates and excellent structural characteristics but also enables artificially specific functions *via* micro- and nanotechnology. Thus, it promotes the development of micro/nanorobots for application in environmental purification, drug delivery, imaging diagnosis, and cancer treatment.^{24,25} Here, we cover the recent progress and application of natural biological materials as biotemplates for developing micro/nanorobots, including the common plant tissues, bacteria, cells, and microalgae available in nature (Scheme 1). Firstly, the advantages of biotemplates, preparation processes and propulsion modes of micro/nanorobot synthesis using biotemplates with different structures are systematically introduced. Secondly, based on the characteristics of biotemplates, their intelligent applications in environmental chemistry and biomedicine are elaborated. Finally, the current problems and challenges in synthesizing intelligent micro/nanorobots are reviewed, and the future development of intelligent micro/nanorobots for intelligent applications is predicted, which provides new prospects for overcoming some urgent challenges in further applications.

2. Fabrication of intelligent micro/nanorobots

Using biotemplates to prepare functional micro/nanorobots has an alluring prospect and more merits than traditional



Scheme 1 Template sources and applications of intelligent micro/nanorobots.



artificial synthetic materials.²⁶ First, biotemplates have the advantages of vast sources, strong renewability, low cost, *etc.*²⁷ Second, natural biotemplates have unique structures, including needle-like biological calcification tubes, sea urchin-like pollen, spherical chlorella, and spiral spirulina. Their unique structure is shown in Fig. 1A. These biotemplates are uniform in shape, widespread and reproducible, and can be directly collected or cultivated from the external environment. For instance, pollen spores, yeast microorganisms, and microalgae with micro/nanosphere characteristics can be obtained through large-scale cultivation.²⁸ However, traditional artificial synthetic materials require a high cost and will discharge pollutants harmful to the environment.²⁹ Third, the surface of a biotemplate is rich in active functional groups, which chemical reactions can modify.³⁰ For example, the cell wall of microalgal cells and yeast is usually composed of cellulose, mannan, dextran, *etc.*, which contain rich glycosidic bonds and

hydroxyl functional groups and can conduct a series of polymerization reactions to introduce specific functional groups.^{20,31} More importantly, chemical reactions can also convert these groups into new active groups. The naturally formed functional groups avoid the use of tedious chemical synthesis steps.¹⁹ Fourth, the thermal stability of a biotemplate is poor and can be volatilized by high-temperature pyrolysis and carbonization without residue.²⁷ Finally, biotemplates, as drug carriers, are non-toxic and harmless to the body and have good biocompatibility.³² It is worth mentioning that living organisms self-propelled micro/nanorobots providing unique advantages for their applications because they can achieve active propulsion without external fuels or energies.^{33,34} In short, biotemplates have attracted more and more attention due to their irreplaceable advantages over other template materials. Therefore, the material sources of intelligent micro/nanorobots were classified in this section.



Fig. 1 Typical structure of natural biotemplates and manufacturing strategies of micro/nanorobots. (A) Natural biotemplates with different structures. (B) A brief description of the fabrication process of micro/nanorobots using natural biotemplates. (C) Fabrication schemes of typical biotemplates used for preparing micro/nanorobots.



The feasibility of the fabrication strategy must be considered when selecting a biotemplate and artificial carriers with specific structures for a specific application. In a comprehensive consideration, the manufacturing strategy is mainly divided into two steps: chemical precipitation and chemical adsorption. The basic process of manufacturing functional micro/nanorobots using a biotemplate is shown in Fig. 1B. First, the target micro/nanomotor is prepared by selecting a specific structure to replicate the template's external shape or internal structure.³⁵ Subsequently, the functional material is loaded on the surface of the micro/nanomotor by artificial modification to achieve specific applications. To better demonstrate the preparation process, two typical biotemplates (sunflower and spirulina) are shown as biotemplates for preparing multifunctional micro/nanorobots. As shown in Fig. 1C, when the sunflower pollen is used as a biotemplate, it is first necessary to obtain individual pollen particles *via* separation, then a layer of metal or metal oxide is deposited on their surface for propulsion, and finally, drugs can be loaded. When spirulina is used as a biotemplate, it can be directly used for preparing micro/nanorobots without pretreatment. Similarly, magnetic metals or metal oxides can be deposited on its surface by chemical deposition, and then drugs can be loaded onto its surface through surface modification to obtain magnetically propelled micro/nanorobots. In recent years, significant progress has been achieved in transforming biotemplates into functional micro/nanorobots, and various natural materials as new material sources have been introduced in several fields of materials science. According to the different sources of biotemplates, they can be roughly divided into four categories. Therefore, this section highlights several common biotemplates used to fabricate intelligent micro/nanorobots and their main preparation processes.

3. Classification of intelligent micro/nanorobots

3.1. Plant tissue-based micro/nanorobots

Functional micro/nanorobots usually use chemical materials as precursors with complex preparation processes and harsh reaction conditions. In addition, it can greatly increase the production cost of the materials and seriously hinder the application of micro/nanorobots to some extent.³⁶ Therefore, seeking resource-rich, inexpensive, and readily available new materials to replace traditional chemical materials is significant for large-scale production of low-cost functional micro/nanorobots. Plants are multicellular eukaryotes, one of the primary forms of life, including trees, shrubs, grasses, ferns, vines, mosses, *etc.* The number of species exceeds 300 000, and they cause no pollution, are easy to obtain, and have highly regenerative characteristics.³⁷ Plant tissues have created uniquely complex patterns and elegant structures over millions of years. They are capable of generating a variety of highly ordered hierarchical structures on different scales, which rival the sophistication of current engineered materials, such as

vessels,¹⁷ calcified crystals,^{38,39} pollen,^{40,41} dandelion fluffs,²¹ fibers.⁴² These plant tissue materials with exotic microstructures are extracted, can be used as substrate materials after artificial treatment and subsequently transformed into functional micro/nanorobots by synthetic manufacturing techniques.²⁰ Next, several typical biotemplates will be shown for preparing plant tissue-based micro/nanorobots.

Vascular plants were rich in uniform spiral microstructures, and can be used to prepare micromotors with efficient propulsion. Gao *et al.* proposed the first example of plant vascular-based bioinspired magnetically propelled helical microswimmers.¹⁷ Due to the extremely high density of spiral vessels within the leaves, over a million individual helical swimmers can be generated from a short single segment of the plant stem (Fig. 2A). Geometric variables of the spiral vessels, such as the helix diameter and pitch, can be controlled by mechanical stretching for the precise fabrication and consistent performance of helical microswimmers. Then, sequential deposition of thin Ti and Ni layers directly on the spiral vessels, followed by dicing, leads to extremely simple and low cost plant vascular-based magnetic microswimmers displaying efficient propulsion, with a speed of over $250 \mu\text{m s}^{-1}$, as well as powerful locomotion in biological media such as human serum. Such a new method of using the spiral plant vessel as the significant component of the helical micromotor dramatically simplifies the fabrication process by utilizing the intrinsic biological microstructures that nature provides. In addition, the helical microstructures derived from the lotus-root fibers can also be used to prepare microswimmers.⁴³ A simple and reproducible method is illustrated in Fig. 2B, and the helical fibers are mechanically isolated from the lotus roots. The whole process proceeds sequentially through cutting, breaking, and stretching. The stretching span in Fig. 2B can be controlled thus tailoring the length of the helices. After that, the obtained helices are subject to the coating of the Fe_3O_4 magnetic layer, and then they are diced into the desirable lengths to enable magnetic actuation. Moreover, this work also reveals that microswimmers with soft bodies could locomote faster than those with rigid bodies, which shows their prospect for biomedical applications in the future.

In nature, sunflower pollen particles with unique microstructures can be used to prepare micro/nanorobots with specific functions. Liu *et al.* fabricated a bioinspired micromotor based on sporopollenin exine capsules (SECs) extracted from sunflower pollen grains which can encapsulate macromolecular compounds for cargo delivery as well as absorb heavy metals for decontamination of water without further functionalization.⁴⁴ As illustrated in Fig. 2C, to demonstrate the encapsulation ability of SECs, bovine serum albumin (BSA) was used as a model biomacromolecule and loaded within the SECs by a vacuum-assisted loading technique. In order to achieve the goal of cargo delivery within the micromotor design framework, a layer of Pt was deposited on one side of the BSA-loaded SECs. The partial Pt layer on the outer surface imparts catalytic properties toward H_2O_2 decomposition to the BSA-loaded SECs, enabling their motion in the presence of a H_2O_2 fuel.





Fig. 2 Plant tissue template-based micro/nanorobots. (A) Bioinspired helical microswimmers based on vascular plants. Reprinted with permission from ref. 17. Copyright 2014 American Chemical Society. (B) Swimming characteristics of bioinspired helical microswimmers based on soft lotus-root fibers from ref. 43. Copyright 2017 Multidisciplinary Digital Publishing Institute. (C) Bioinspired spiky micromotors based on sporopollenin exine capsules from ref. 44. Copyright 2017 Wiley-VCH. (D) Bioinspired zeolitic imidazolate framework (ZIF-8) magnetic micromotors for highly efficient removal of organic pollutants from water from ref. 42. Copyright 2019 Elsevier.

The biocompatibility and large internal cavities of SECs make them suitable for encapsulation and delivery of cargo. The porous polymeric structure and functional groups on the surface offer sporopollenin the ability to absorb heavy metals without any additional modification. By harnessing the advantageous features of SECs, such micromotors open new horizons for using plant pollen-derived materials to address biomedical and environmental issues.

Natural kapok fibers have unique hollow structures, inspiring the design and fabrication of bubble-driving tubular micromotors. Liu *et al.* first demonstrated novel self-propelled Pt-free ZIF-8 magnetic micromotors using a bio-inspired approach as an active adsorbent for highly efficient wastewater treatment.⁴² The fabrication process of micromotors is illustrated in Fig. 2D. Briefly, the kapok fiber was used as the template first to fabricate mixed metal oxide ($\gamma\text{-Fe}_2\text{O}_3/\gamma\text{-Al}_2\text{O}_3$) magnetic porous microtubes. Then catalytic material MnO_2 particles were synthesized on the microtubes' outer and inner surfaces. Subsequently, ZIF-8 was loaded on the outer side of the above-mentioned magnetic tubes *via in situ* growth. After that, the catalytic layer was only exposed on the inner surface of the microtube, and the final tubular ZIF-micromotors were obtained. In the presence of a fuel (H_2O_2), the micromotors will be driven by the O_2 bubbles and finally cause efficient

dynamic adsorption toward pollutants in water. In this, the micromotors prepared by the kapok template method retained the natural asymmetric hollow fiber structure of kapok that provides unbalanced force conditions without further complex procedures.

3.2. Cell-based micro/nanorobots

Most micro/nanorobots obtained from plant tissue templates are rigid. Therefore, creating soft and flexible micro/nanorobots is meaningful because the ability to change shape allows movement through tight spaces or winding channels, enabling specific applications.^{45,46} Nature provides myriad sophisticated biological cells (such as red blood cells and sperm cells) that can display and regulate motion in well-established manners over long ages of evolution.² They have received substantial interest as model carriers due to their abundance, biocompatibility, biodegradability, non-immunogenicity, inert intracellular environment, and ease of handling.⁴⁷ More importantly, in soft micro/nanorobots, cell-based micro/nanorobots constructed by the integration of living cells and flexible materials have reproduced similar organ or tissue construction and functions of organisms. This integration is attributed to the progress of manufacturing technologies and advances in tissue engineering. Compared with traditional rigid micro/nanorobots, cell-based micro/nanorobots



exhibit superiority in intrinsic softness, environmental safety and compatibility, remarkable energy conversion efficiency, and integrated sensing and control.⁴⁸ Furthermore, some cells can direct and transport various synthetic organic/inorganic functional payloads through functionalization with intrinsic chemotactic behavior, thereby generating carrier-cell interactions without mechanical damage, which is critical for biomedical applications.⁴⁹ Based on these, cells are promising in designing and fabricating various types of bionic delivery robots due to their natural advantages.⁵⁰ Synthetic micro/nanorobots are envisioned to move, sense, and perform specific functions like their biological counterparts.⁵¹ Below, we present several examples of micro-robots using cells as substrate materials for synthesizing microrobots.

Red blood cells (RBCs) are of particular interest owing to their vast availability, unique mechanical attributes, surface

immunosuppressive properties, and versatile cargo-carrying capability. Wu *et al.* reported an RBC-derived approach for developing a new generation of cell-based micromotor powered by ultrasound and activated by a magnetic field.⁵² Fig. 3A shows the preparation of magnetically guided, ultrasound-propelled RBC micromotors. Initially, citrate-stabilized magnetic Fe_3O_4 nanoparticles were synthesized. Then, the fresh RBCs were collected from mice and anticoagulated with ethylenediamine tetraacetate. Finally, a RBC micromotor was prepared using a hypotonic dilution/encapsulation method to load iron oxide nanoparticles (20 nm) into RBCs. The RBC micromotor was propelled by the pressure gradient generated by the ultrasound waves due to the inherent asymmetric geometry of the RBCs as well as the asymmetric distribution of magnetic particles inside the RBCs. Owing to their inherent biomimetic properties, these new RBC micromotors are not susceptible to macrophage

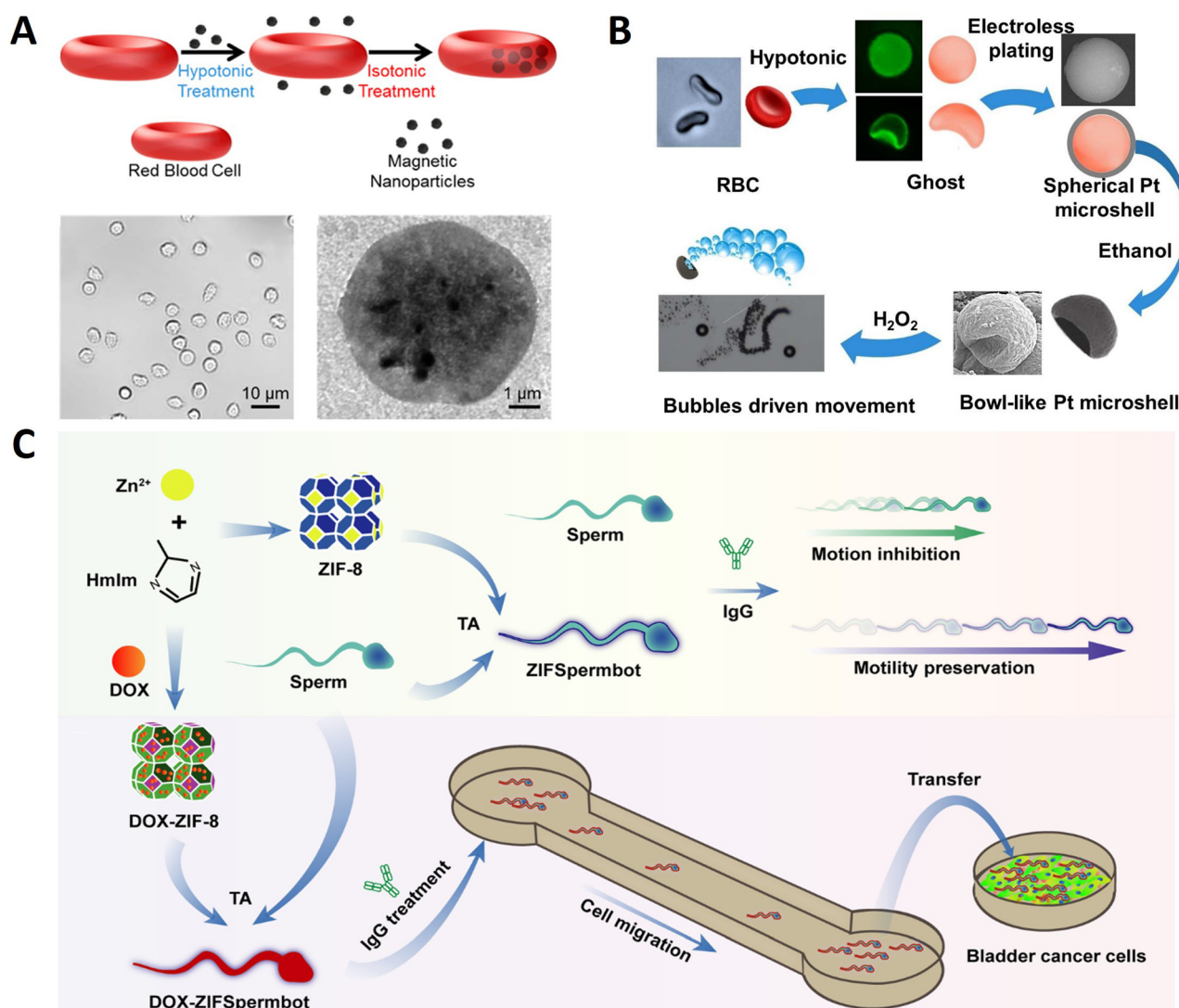


Fig. 3 Cell template-based micro/nanorobots. (A) Turning erythrocytes into functional micromotors. Reprinted with permission from ref. 52. Copyright 2014 American Chemical Society. (B) Bowl-like micromotors using red blood cell membranes as a template. Reprinted with permission from ref. 54. Copyright 2019 Wiley-VCH. (C) Multifunctional metal-organic framework exoskeletons protect biohybrid sperm microrobots for active drug delivery from the surrounding threats. Reprinted with permission from ref. 55. Copyright 2021 American Chemical Society.



uptake, displaying remarkable biocompatibility essential for practical biomedical uses.

The RBC membrane is the hollow ghost that RBCs obtain through hemolysis. It can form a natural compartment to protect internal materials and couple therapeutic molecules for various delivery applications, making it widely used in the surface modification of nanoparticles.⁵³ RBC membranes with good deformability and fluidity are excellent natural templates for micromaterial fabrication. Pan *et al.* used RBC membranes as templates to prepare asymmetric Pt bowl-like micromotors responsive to H₂O₂ (Fig. 3B).⁵⁴ The red blood cells were collected from a healthy donor, and then hemoglobin was removed by hemolytic swelling to obtain a single-sided concave shape ghost. Subsequently, the ghost was used as a template to prepare bowl-like micromotors by electroless plating of platinum particles onto the membranes. Due to the shrinkage of the internal template and the softness of the platinum shell, the products deformed from the spherical structure to a bowl-like structure with treatment. The recessed portion of the platinum bowl structure has a negative curvature to generate oxygen bubbles, which generates a one-way driving force to push the micromotor forward. These asymmetric bowl-like micromotors are expected as cargoes for drug delivery.

Mammalian sperm cells have strong propulsion, chemotactic behavior, and immune evasion capabilities that are highly advantageous in building sperm-based micro-robots. As shown in Fig. 3C, Pan *et al.* reported sperm-driven biohybrid microrobots.⁵⁵ Doxorubicin (DOX) was encapsulated in ZIF-8 NPs through the *in situ* biomineralization method to obtain DOX-ZIF-8 NPs. In order to build DOX-ZIFspermbot, sperms were mixed with DOX-ZIF-8 NPs and tannic acid (TA) was added to induce the complexation between ZIF-8 and the cell membrane. Combining the effective protection of sperm propulsion with the drug-loading capacity of ZIF-8 NPs provides new applicability to ZIFspermbots in risky surroundings with AsA, exhibiting rapid migration in a microfluidic device for active drug delivery with enhanced therapeutic efficacy due to their retained effective propulsion. Utilizing spermatozoa as the engine unit of robotic systems at a microscale has revolutionized inspirations and strategies for the biomedical community.

3.3. Microalgae-based micro/nanorobots

Microalgae are photosynthetic unicellular microorganisms and widely exist in nature.⁵⁶ They grow rapidly, simple in structures, adaptable to different environments, and have excellent biocompatibility and biodegradability.⁵⁷ Microalgae produce a variety of compounds, such as photosynthetic pigments (carotenoids and chlorophylls), sterols, polyunsaturated fatty acids, vitamins, minerals, fibers, polysaccharides, enzymes, peptides, and toxins which have broad applications in many fields.^{58,59} They have attracted great interest in recent years due to their potential applications in nutraceutical and pharmaceutical industries, and are a major source of food, energy, health, environment, and biomaterials.⁶⁰ Microalgae can rapidly proliferate and be obtained in large quantities through artificial

cultivation and can be used as biotemplate without treatment.⁶¹ Micro/nanorobots with special structures and functionalities can be obtained by depositing or loading *via* using microalgae as biotemplates.⁶² The strange shapes of microalgae, such as spherical, triangular, elliptical, star-shaped, and other irregular shapes, provide ideas for preparing microalgae-based micro/nanorobots with specific structures for specific applications.⁶³ Therefore, using microalgae as substrate materials enables the controlled synthesis of functional micro/nanorobots with specific morphology and microstructure.⁶⁴ At the same time, using biomaterials rich in elements and chemical components related to life activities to achieve a full range of biotemplates is a major advantage unmatched by other artificially engineered templates.^{65,66} Here, several typical examples of preparing microalgae-based micro/nanorobots using microbial algae as templates will be introduced.

Chlorella pyrenoidosa (*C. pyrenoidosa*) has uniform spheroidal structures with diameters around 3–5 μm, even smaller than those of human red blood cells. These fascinating features give them the superiority to act as ideal natural biomaterials for biomedical applications. Liu *et al.* fabricated a bioinspired micromotor to precisely activate muscle.⁶⁷ As displayed in Fig. 4A, *C. pyrenoidosa* was used as a biotemplate to prepare magnetic microswimmers *via* a facile dip-coating approach. In this fabrication process, *C. pyrenoidosa* and the Fe₃O₄ nanoparticles were oppositely charged so that discrete Fe₃O₄ nanoparticles could be effectively absorbed on the surface of *C. pyrenoidosa* and grow. Under the wireless actuation of a weak rotational magnetic field, the engineered biohybrid microswimmers could navigate and follow complex trajectories *in vitro*. Meanwhile, the single microswimmer could approach targeted derived myotube accurately by remote manipulation and then efficiently induce myotube contraction under NIR stimulation, with a local temperature increase of approximately 5 °C. The as-developed magnetically actuated microswimmer-based strategy can provide a renovation for tissue engineering and bionics.

Diatoms have a well-defined cell wall known as a frustule, made up of SiO₂, Al₂O₃, and Fe₂O₃, which can act as a catalyst and provide thrust in solution. As shown in Fig. 4B, Panda *et al.* report a novel bio-inspired approach for preparing self-propelled micromotors by catalytic decomposition of H₂O₂ as a fuel.⁶⁸ The diatoms are composed of a silicate backbone with biological moieties containing organic molecules and trace amounts of metal ions, such as those of iron. Interestingly, a trace amount of iron oxide (Fe₂O₃) in the diatom was converted into Fe₃O₄, which can act as a catalyst to achieve the facile decomposition of H₂O₂ and unidirectional motion. The unique 3D hierarchical structure of the diatom can provide the bubbling force anisotropically in solutions, resulting in unidirectional motion for diatom-based micromotors. These frustules are mechanically robust, chemically balanced, and eco-friendly; thus, they can easily be used in biological and environmental applications.

Chlamydomonas reinhardtii (*C. reinhardtii*) presents intriguing biological swimmers with high propulsion, autofluorescence,





Fig. 4 Microalgal template-based micro/nanorobots. (A) Magnetically actuated biotemplate-based microswimmers for precise photothermal muscle contraction. Reprinted with permission from ref. 67. Copyright 2022 American Chemical Society. (B) Bio-inspired self-propelled diatom micromotors obtained by catalytic decomposition of H_2O_2 at low fuel concentration. Reprinted with permission from ref. 68. Copyright 2018 Royal Society of Chemistry. (C) Microalga-powered biohybrid microswimmers for active cargo delivery. Reprinted with permission from ref. 69. Copyright 2018 Wiley-VCH. (D) Facile fabrication of magnetic microrobots based on spirulina templates for targeted delivery and synergistic chemo-photothermal therapy. Reprinted with permission from ref. 70. Copyright 2019 American Chemical Society.

and phototactic guidance capabilities. Inspired by this, Yasa *et al.* developed a biocompatible biohybrid microswimmer powered by *C. reinhardtii* as shown in Fig. 4C.⁶⁹ This biohybrid algal microswimmer comprises an intact microalga, *C. reinhardtii*, attached to the polyelectrolyte (PE) functionalized 1 μm diameter magnetic polystyrene (PS) particles. Cargos were noninvasively attached to the microalgae without compromising the natural motility, using noncovalent electrostatic interactions between the positively functionalized magnetic PS microparticles and the negatively charged microorganisms. As a result, the biological segment of the biohybrid microswimmers serves as an actuator and sensor, while their artificial segment provides support and other functionalities. Similarly, using natural swimmers as cargo delivery agents presents an alternative strategy to transport therapeutics inside the body to locations otherwise difficult to access by traditional delivery strategies.

Helical magnetic microrobots have attracted particular attention because they can transform the rotation around their helical axis into a translational motion along the helical axis to provide an efficient and precise 3D locomotion behavior. As shown in Fig. 4D, Wang *et al.* proposed a facile method for the mass production of magnetic microrobots with multiple functions using *Sp.* as a biotemplate.⁷⁰ Initially, the Pd@Au core-shell NPs were embedded both in the *Sp.* cells and on the cell walls. Subsequently, Fe_3O_4 NPs are deposited on the as-prepared (Pd@Au)@*Sp.*, enabling the obtained (Pd@Au)/ Fe_3O_4 @*Sp.* microrobots to be actuated in an external magnetic field. Finally, chemotherapeutic doxorubicin (DOX) is loaded to

obtain (Pd@Au)/ Fe_3O_4 @*Sp.*-DOX microrobots. They can elide the process of fabricating spiral configuration by taking advantage of their intrinsic helical morphology compared to other manufacturing methods of microrobots. Furthermore, the helical structure endows the as-prepared microrobots with efficient propulsion performance with the highest speed of $526.2 \mu\text{m s}^{-1}$ under a rotating magnetic field. Such facile fabrication of magnetic microrobots based on *Sp.* as a template is very promising.

3.4. Bacterial template-based micro/nanorobots

Microorganisms such as bacteria have good micro-organic structures and small sizes, and can be used as templates to synthesize nanostructured materials⁷¹ because bacteria have evolved many dominant structural biological forms in continuous evolution and can precisely control these morphological structures at the nanometer level through their regulatory mechanism. Current scientific and technological means make it difficult to prepare ordered 3D nanospheres, but bacteria such as cocci and helicobacter can easily form such structures. Therefore, using bacteria as templates has the advantages of wide access and potential gene regulation functions, and has a good application prospect.⁷² Additionally, bacteria have a high swimming speed and efficiency in the low Reynolds (Re) number flow regime, can sense and respond to external environmental signals, and can be externally detected *via* fluorescence or ultrasound imaging techniques.^{25,73} In particular, bacteria offer several advantages as controllable microactuators: they draw chemical energy directly from their environment,



they can be genetically engineered and employed as sensing elements and they are scalable and configurable in that the bacteria can be selectively patterned.⁷⁴ Due to their inherent advantages, various bacteria (*Escherichia coli*,²⁵ *Magnetotactic bacteria*,⁷⁵ *Salmonella typhimurium*,⁷⁶ etc.) have been used as carriers to prepare as potential microrobots. Next, a few examples are introduced.

Bacteria can be integrated with synthetic substances to produce multiple functionalities through their biological actuation and sensing capabilities. Buss *et al.* present a biohybrid microswimmer composed of a genetically engineered peritrichously flagellated *Escherichia coli* species integrated with red blood cell (RBC) derived nanoliposomes.²⁵ As displayed in Fig. 5A, firstly, the genetically engineered bacterial species were induced with isopropyl-*b*-D-thiogalactopyranoside (IPTG) to obtain bacterial species with biotin molecules on their cell membranes. Then, RBCs were isolated from whole murine blood, and nanoerythrocytes were fabricated from emptied RBCs using the cell extrusion technique. The nanoerythrocytes were modified with biotin molecules *via* biotin-conjugated anti-TER119 antibodies to realize the non-invasive conjugation of the bacterial actuators with the cargo carriers. Finally, microswimmers were constructed by conjugating streptavidin-modified bacteria with biotin-modified nanoerythrocytes using non-covalent streptavidin interactions. These microswimmers showed enhanced swimming speeds compared to the previously reported biotemplate-based microswimmer

designs powered by various *Escherichia coli* strains. Besides, more applications could be achieved by rational design of bacteria's surface. Chen *et al.* designed a biohybrid microrobot able to move by applying a magnetic field and in thermal and hypoxic environments, integrating the properties of both magnetic nanoparticles (MNPs) and *Escherichia coli* Nissle1917.⁷⁷ In order to achieve imaging-guided magnetothermal treatment, genetically engineered probiotics were prepared using pBV220 expression vectors encoded with the NDH-2 or mCherry/NDH-2 gene sequences, and the thermally sensitive promoter TcI was integrated. Then, bacterial hybrid microrobots were prepared by conjugating the Zn-doped Fe₃O₄ MNP (Zn_{0.4}Fe_{2.6}O₄) on the genetically engineered probiotics (Fig. 5B). Compared with artificial micro/nanorobots, the bacteria endow microrobots with efficient self-propulsion, and integration of the physical, biological and chemical properties, enabling microrobots with triple sensing capabilities of magnetism, heat, and hypoxia to overcome harsh biological environments and achieve satisfactory therapeutic effects.

Magnetococcus marinus strain, magnetospirillum magneticum (AMB-1), can be used to prepare intelligent biotemplate-based microbiorobotics due to its magnetosomes inside the body being susceptible to external magnetic fields. Xing *et al.* developed an AI microrobot system using AMB-1 as the template composed of motile AMB-1 and light-triggered indocyanine green nanoparticles (INPs).⁷⁸ The INPs were synthesized with maleimide groups in the phospholipid shell and ICG in



Fig. 5 Bacterial template-based micro/nanorobots. (A) Nanoerythrocyte-functionalized biohybrid microswimmers. Reprinted with permission from ref. 25. Copyright 2019 AIP Publishing. (B) An engineered bacteria-hybrid microrobot with a magnetothermal bioswitch for remotely collective perception and imaging guided cancer treatment. Reprinted with permission from ref. 77. Copyright 2022 American Chemical Society. (C) Sequential magneto-actuated and optics-triggered biomicrorobots for targeted cancer therapy from ref. 78. Copyright 2021 Wiley-VCH. (D) Magnetic torque-driven living microrobots for increased tumor infiltration. Reprinted with permission from ref. 75. Copyright 2022 AAAS.

the poly(lactic-co-glycolic acid) (PLGA) core by a single-step sonication method. In parallel, surface protein disulfides of AMB-1 were reduced to activated sulfhydryl by tris(2-carboxyethyl) phosphine (TCEP). Finally, the INPs were chemically conjugated onto the activated sulfhydryl outside the AMB-1 membrane by a Michael addition reaction to form a smart AI microrobot (Fig. 5C). Such AI microrobots with autonomous flagellum propulsion can realize controlled navigation, focal localization, deep penetration, and tumor colonization *in vivo*. Therefore, bacteria-based microrobots were increasingly recognized as promising externally controllable vehicles for targeted cancer therapy. As shown in Fig. 5D, Gwisai *et al.* reported magnetic torque-driven living microrobots for increasing tumor infiltration using *magnetospirillum magneticum* as a magnetically responsive model organism.⁷⁵ Bioconjugation was achieved through carbodiimide coupling using an adapted protocol. Briefly, activation of carboxylated liposomes was accomplished by incubating 300 μ L of liposome solution with EDC and sulfo-NHS for 20 min in PBS at room temperature with gentle agitation. The activated liposomes were subsequently incubated with *magnetotactic bacteria* (MTB) cells for 2 h at room temperature with gentle agitation. Unbound liposomes were separated from MTB-liposome conjugates (MTB-LP) using a 2D magnetic field. By merging the benefits of bacteria-mediated therapy with a scalable magnetic torque-driven control strategy, their approach enables effective, targeted delivery of living microrobots for improved treatment. A fourfold increase in translocation of magnetically responsive bacteria across a model of the vascular endothelium observed is attributed to torque-driven surface exploration at the cell interface.

4. Applications

Preparing intellect micro/nanorobots using biotemplates has excellent application prospects. On the one hand, creatures in nature have evolved various structures to adapt to external stimuli, and the size and morphology of these structures are very regular. Using these structures as biotemplates introduces the “smart” function of biological hybrid materials and avoids the waste of chemical materials.⁷⁹ On the other hand, the surface of biotemplates contains wealthy modifiable functional groups, which can be used to prepare functional materials that meet the needs of chemical reactions to connect special functional groups or change their hydrophobicity.^{31,80} More importantly, different structures of natural biotemplates give various intelligent applications to micro/nanorobots.⁸¹ For example, large internal cavity pollen grains are ideal for drug or nanoparticle encapsulation,⁸² calcified porous microneedles were used for cell-microdrilling,³⁹ hollow kapok fiber provides unbalanced force conditions in the motion,⁸³ and helical structures can convert rotational motion to translational motion.⁸⁴ Therefore, through appropriate design and assembly, environmentally friendly, cheap, readily available biotemplates and specific functional chemical components can be used in complex and diverse intelligent applications, such as removal of organic

pollutants, biosensors, and cancer treatment.^{85,86} This part mainly introduces the application of intelligent micro/nanorobots in the environment and biology. Owing to the large variety of biotemplates and the multitude of nanomedicines that have been developed using different materials, structures, coatings, and functional ions, biotemplate-based micro/nanorobots can be combined in a plethora of configurations allowing their tailoring to achieve specific applications defined by the nature of the targeted objects and their microenvironment.⁴⁶ Thus, a summary of representative examples of various nature-/structure-inspired micro/nanorobots is presented in Table 1.

4.1. Biomedical applications

4.1.1. Drug delivery. Although remarkable achievements in active cargo delivery have been made over the past decade, delivery systems based on micro/nanorobots are still limited by complex physiological conditions *in vivo*.¹⁴² When exposed to body fluids, the existing microrobot systems may compromise their structures and functions, let alone the encapsulated therapeutic drugs.¹⁴³ Besides, large-scale inexpensive production of micro/nanorobots with high biocompatibility and excellent physicochemical robustness is always challenging. A micro/nanomotor made from a biotemplate is expected to overcome this difficulty because of its good biocompatibility and surface-modifiable functional groups.²⁷ Moreover, performing the on-demand release of the maximum amount of the loaded drug at a specific position is particularly imperative.⁶⁴ Here, the self-propelled bio-based micro/nanorobots provide the carriers with continuous driving power to help them transport across biological tissues. In addition, the direction of the micro/nanorobots can also be adjusted to prompt cell targeting and internalization to enhance the controllability and adjustability of the drug delivery system. Compared to passive drug carriers, the self-propulsion abilities of these biotemplate-based micro/nanorobots have unique advantages in drug delivery, which bring distinct improvements for efficient drug delivery.

A significant advantage of using a biotemplate is that contrary to elaborate clean-room fabrication techniques, a large amount of material can be obtained relatively quickly with minimal process control. As displayed in Fig. 6A, Sarvesh *et al.* extracted calcified porous microneedles (40–60 μ m long) from the *Dracaena sp.* plants that possess drug carrier capability (much like calcium-based drug carriers) and coated these structures with a magnetic layer to facilitate cellular drilling due to its microneedles structure by external magnetic actuation.³⁹ Subsequently, loading these calcified biotubes with the anticancer drug camptothecin allows for the site-specific activation of the drug in the acidic environment of HeLa cancer cells. These elongated porous microneedles were used to prepare magnetic biogenic microdaggers that can be used as daggers with microdrilling capability for piercing cells, but also with additional advantages of drug release function, due to which they can be used as a “cell microsurgery and drug rehabilitation” package.

Pollen, a renewable biomaterial that exists in nature widely, has a unique architecture, excellent biocompatibility, structural uniformity, good permeability, and a large hollow cavity. These



Table 1 A summary of biotemplate-based intelligent micro/nanorobots

| Natural structure | Main components | Speed ($\mu\text{m s}^{-1}$) | Propulsion mechanism | Applications | Ref. |
|-------------------------------|--|--------------------------------|----------------------|---|------|
| Plant tissue | | | | | |
| Leave vessels | Vessels/Ti/Ni | 250 | Magnetic field | — | 17 |
| Banana leaf vessels | Vessels/Ni/Fe ³⁺ -TA | 51 | Magnetic field | Degradation of RhB and capture of cells | 87 |
| Lotus-root fibers | Fibers/Fe ₃ O ₄ | — | Magnetic field | — | 43 |
| Tomato callus | Callus/Fe ₃ O ₄ | 6.23 | Magnetic field | Removal of chlorpyrifos | 88 |
| Tomato callus | Callus/Fe ₃ O ₄ /Vitamin C | — | Magnetic field | Cell clones | 89 |
| Kapok fibers | Fibers/ γ -Fe ₂ O ₃ / γ -Al ₂ O ₃ /MnO ₂ /ZIF | ~150 | Chemical reaction | Adsorption of organic pollutants | 42 |
| Kapok fibers | Fibers/Eu-MOF/EDTA-NiAl-CLDH-M | 56.9 | Chemical reaction | Sensing and removal of Fe ³⁺ | 83 |
| Lotus pollens | Pollen/MnO ₂ /CoFe ₂ O ₄ | ~116 | Chemical reaction | Recognition and capture of Pb ²⁺ | 90 |
| Chrysanthemum pollen | Pollen/Fe ₃ O ₄ /DOX | 400 | Magnetic field | Tumor assassination and tissue regeneration | 82 |
| Lotus pollen | Pollens/PNIPAM/Mn ₃ O ₄ /CoFe ₂ O ₄ | 161 | Chemical reaction | Adsorption of erythromycin | 91 |
| Pine pollen | Pollen/Fe ₃ O ₄ /DOX | 175.19 | Magnetic field | Drug delivery | 92 |
| Sunflower pollen | Pollen/Fe ₃ O ₄ /Galinstan-Fe alloy | ~90 | Magnetic field | Eradicate biofilm | 93 |
| Sunflower pollen | Pollen/polydopamine | 1000 | Light | Capture and transport of yeast cells | 94 |
| Sunflower pollen | Pollen/polydopamine/vancomycin | — | Light | Capturing and killing targeted bacteria | 95 |
| Sunflower pollen | Pollen/Au/Co/DOX | ~25 | Magnetic field | Attract, manipulate and kill cancer cells | 96 |
| Sunflower pollen | Pollen/Ni | 110 | Magnetic field | Removal of oil and microplastics | 97 |
| Sunflower pollen | Pollen/Ni/Ti/DOX | 125 | Magnetic field | Intracellular delivery | 98 |
| Sporopollenin exine capsules | Sporopollenin/BSA/Pt | 90.83 | Chemical reaction | Drug delivery and removal of Pb ²⁺ | 44 |
| Cell | | | | | |
| Calcified biotubes | Biotube/Fe-Ti/camptothecin | — | Magnetic field | Single-cell surgery, drug release | 39 |
| Red blood cell(RBC) | RBC/Fe ₃ O ₄ | 16 | Ultrasound | Anti-biological pollution | 52 |
| Erythrocytes | Erythrocytes/magnetic beads | ~4 | Magnetic field | — | 99 |
| Bovine sperm cell | Sperm cell/Fe ₃ O ₃ /DOX | 12.5 | Magnetic field | Drug loading | 100 |
| Bovine sperm cell | Sperm cell/Fe/DOX | — | Magnetic field | Drug loading and ultrasound imaging | 101 |
| Bovine sperm cell | Sperm cell/iron oxide/polystyrene | 121.1 | Self-propulsion | Assisted reproduction | 102 |
| Human sperm cell | Sperm cell/Fe-Ti/DOX/camptothecin | — | Magnetic field | 3D ovarian cancer cell treatment | 103 |
| Human sperm cell | Sperm cell/ZIF-8/DOX/TA | 73 | Self-propulsion | Active drug delivery | 55 |
| Ciona sperm cell | Sperm cell/Fe ₃ O ₃ /DOX | 217 | Self-propulsion | Drug loading capacity and responsive release | 104 |
| | Sperm cell/CdSe/ZnS | — | — | — | — |
| | Sperm cell/Pt/FTTC | — | — | — | — |
| Clarias gariepinus sperm cell | Aqua sperm cells | 114 | Self-propulsion | Removal of bacterial biofilms | 105 |
| Red blood cell membrane | RBC membrane/Pt | 686 | Chemical reaction | — | 54 |
| Microalgae | | | | | |
| Chlorella | Chlorella/Fe ₃ O ₄ | ~17 | Magnetic field | Precise photothermal muscle contraction | 67 |
| Chlorella | Chlorella/Fe ₃ O ₄ /BiOCl | 80.45 | Magnetic field | Degradation of RhB and bacterial inactivation | 106 |
| Chlorella | Chlorella/Fe ₃ O ₄ /BiOx | 40 | Magnetic field | Degradation of dyes and pollutants | 107 |
| Chlorella | Chlorella/Fe ₃ O ₄ /ZIF-8 | 40.2 | Magnetic field | Antibacterial treatment | 108 |
| Chlorella | Chlorella/Fe ₃ O ₄ /DOX | 107.6 | Magnetic field | Targeted drug delivery | 109 |
| Chlorella | Chlorella/Fe ₃ O ₄ | 35 | Magnetic field | Removal of micro/nanoplastics | 110 |
| Spirulina | Spirulina/Fe ₃ O ₄ /MnO ₂ | 250 | Magnetic field | Removal of Pb(ii) | 111 |
| Spirulina | Spirulina/Fe ₃ O ₄ /FTTC-BSA | — | Magnetic field | Molecular cargo delivery | 64 |
| Spirulina | Spirulina/Fe ₃ O ₄ /CuS | 583.3 | Magnetic field | Anticancer therapy and bacterial killing | 112 |
| Spirulina | Spirulina/Fe ₃ O ₄ /PDA | 123.84 | Magnetic field | Pathogenic bacterial infection treatment | 113 |
| Spirulina | Spirulina/Fe ₃ O ₄ | 15.2 | Magnetic field | Bacterial killing | 114 |
| Spirulina | Spirulina/Fe ₂ O ₃ /MIL-125NH ₂ | ~28 | Magnetic field | Drug delivery and degradation of RhB | 115 |
| Spirulina | Spirulina/Fe ₃ O ₃ /UiO-66 | — | — | — | — |
| Spirulina | Spirulina/Fe ₃ O ₃ /ZIF-8 | — | — | — | — |
| Spirulina | Spirulina/Fe ₃ O ₃ /MIL-100(Fe) | — | — | — | — |
| Spirulina | Spirulina/Fe ₃ O ₄ /MoS ₂ /AuNPs | — | — | — | — |
| Spirulina | Spirulina/Fe ₃ O ₄ /BaTiO ₃ | 68.5 | Magnetic field | Cancer ablation | 116 |
| | | | Magnetic field | Inducing neural stem cell differentiation | 117 |



Table 1 (continued)

| Natural structure | Main components | Speed ($\mu\text{m s}^{-1}$) | Propulsion mechanism | Applications | Ref. |
|---------------------------------|---|--------------------------------|----------------------|---|------|
| Spirulina | Spirulina/Fe ₃ O ₄ /Pd/Au/DOX | 526.2 | Magnetic field | Targeted delivery and chemo-photothermal therapy | 70 |
| Spirulina | Spirulina/Fe ₃ O ₄ | 78.3 | Magnetic field | Cancer therapy | 118 |
| Spirulina | Spirulina/Fe ₃ O ₄ | ~90 | Magnetic field | Imaging-guided cancer therapy | 119 |
| Chlamydomonas pilschmannii | <i>C. pilschmannii</i> | 105 | Self-propulsion | Biomedical operations | 120 |
| Chlamydomonas reinhardtii | <i>C. reinhardtii</i> /PLGA/Dil/DiO | 104.6 | Self-propulsion | Treatment of bacterial pneumonia | 121 |
| Chlamydomonas reinhardtii | <i>C. reinhardtii</i> /vancomycin/ciprofloxacin | 61.5 | Self-propulsion | Against bacterial infections | 122 |
| Chlamydomonas reinhardtii | <i>C. reinhardtii</i> /Fe ₃ O ₄ /chitosan/DOX | 56.3 | Self-propulsion | Cargo delivery | 123 |
| Chlamydomonas reinhardtii | <i>C. reinhardtii</i> | 52 | Light | Cargo delivery and therapy | 124 |
| Chlamydomonas reinhardtii | <i>C. reinhardtii</i> | 100 | Self-propulsion | Picking up and transport cargo | 125 |
| Chlamydomonas reinhardtii | <i>C. reinhardtii</i> | 95 | Light | Manipulation and disruption of biological targets | 65 |
| Chlamydomonas reinhardtii | <i>C. reinhardtii</i> /PS/polyelectrolyte | 162.05 | Self-propulsion | Cargo delivery | 69 |
| Chlamydomonas reinhardtii | <i>C. reinhardtii</i> /chitosan/heparin | 33.3 | Self-propulsion | Diabetic wound healing | 126 |
| Chlamydomonas reinhardtii | <i>C. reinhardtii</i> /vancomycin derivative 7 | — | Self-propulsion | Antibiotic drug delivery | 127 |
| Chlamydomonas reinhardtii | <i>C. reinhardtii</i> /NHS-DBCO/ACE2 | 108 | Self-propulsion | Removal of SARS-CoV-2 | 128 |
| Euglena gracilis | Euglena gracilis | 60 | Light | Drug delivery, removal of apoptotic cells, and photodynamic therapy | 129 |
| Thalassiosira weissflogii | TWFS/Fe ₃ O ₄ /DOX | 28 | Magnetic field | Target therapy | 130 |
| Phaeodactylum tricornutum | Phaeodactylum tricornutum | 209 | Light | Trapping and removal of biothreats | 66 |
| Phaeodactylum tricornutum | Phaeodactylum tricornutum bohlin | 50 | Chemical reaction | — | 68 |
| Diatoms | Diatom | ~90 | Magnetic field | Imaging and therapy | 131 |
| Volvox | Volvox/Fe ₃ O ₄ /PDA/Ce6/chitosan | 30 | Self-propulsion | Cytoprotection and drug delivery | 132 |
| Escherichia coli | <i>E. coli</i> /ZIF-8/DOX/TA | 6.5 | Self-propulsion | Cargo delivery | 133 |
| Escherichia coli | <i>E. coli</i> /dye/streptavidin | 11.7 | Self-propulsion | Targeted drug delivery | 134 |
| Escherichia coli | <i>E. coli</i> /antibody | 18.5 | Magnetic field | Stimuli-responsive cargo delivery | 135 |
| Escherichia coli | <i>E. coli</i> /Fe ₃ O ₄ /nanoliposomes/DOX/ICG | 14.06 | Self-propulsion | — | 25 |
| Escherichia coli | <i>E. coli</i> /nanocerithosomes | 22.5 | Magnetic field | Targeted drug delivery | 136 |
| Escherichia coli | <i>E. coli</i> /PEM/Fe ₃ O ₄ /DOX | 24.62 | Magnetic field | Cancer treatment | 77 |
| Escherichia coli | <i>E. coli</i> /plasmid/MNP | 4.7 | Self-propulsion | Sensing | 137 |
| Bacillus subtilis (B. subtilis) | <i>B. subtilis</i> /cell membrane | 49 | Magnetic field | Increase tumor infiltration | 75 |
| Magnetotactic bacteria (MTB) | MTB/liposome | 13.3 | Magnetic field | Cancer therapy | 78 |
| Magnetotactic bacteria | MTB/ICG | 47 | Self-propulsion | — | 138 |
| Flagellated bacteria | Bacteria | ~23 | Magnetic field | Remote detection of toxins | 139 |
| Ganoderma lucidum spore | Spore/Fe ₃ O ₄ /QDs | 3 | Magnetic field | Targeted delivery | 140 |
| Ganoderma lucidum spore | Spore/Fe ₃ O ₄ /CDs | 266.3 | Magnetic field | Adsorption and removal of heavy metal ions | 141 |





Fig. 6 Bi-template-based micro/nanorobots for drug delivery. (A) Dual-action biogenic microdaggers for single-cell surgery and drug release. Reprinted with permission from ref. 39. Copyright 2016 Wiley-VCH. (B) Magnetic biohybrid micromotors with high maneuverability for efficient drug loading and targeted drug delivery. Reprinted with permission from ref. 92. Copyright 2019 Royal Society of Chemistry. (C) Magnetically steerable bacterial microrobots moving in 3D biological matrices for stimuli-responsive cargo delivery. Reprinted with permission from ref. 135. Copyright 2022 AAAS. (D) A diatom-based biohybrid microrobot with a high drug-loading capacity and pH-sensitive drug release for target therapy. Reprinted with permission from ref. 130. Copyright 2022 Elsevier.

fascinating properties enable pollen to become promising biotemplates for biomedical applications. Sun *et al.* developed pine pollen-based micromotors for targeted drug release, which provide excellent maneuverability in multiple media, efficient drug encapsulation, and on-demand release (Fig. 6B).⁹² These versatile biohybrid micromotors were synthesized for simultaneously encapsulating magnetic particles and drugs into the two hollow air sacs of pine pollen *via* vacuum loading. The micromotors show controllable and continuous locomotion trajectories in complex biological fluids, even on biological tissues (mouse small intestine). Besides displaying controlled propulsion, these micromotors also exhibit a specific mechanism to release therapeutic drugs on demand. Considering the magnetic nanoparticle aggregation phenomenon under a powerful magnetic field, controlled release of a therapeutic cargo is achieved using the fluid field generated by the rotating magnetic agglomeration under a high magnetic field frequency input, which holds great promise for *in vivo* medical applications.

Bacteria-based microrobots, composed of self-propelling bacteria carrying micro/nanoscale materials, can deliver their payload to specific regions under magnetic control, enabling additional effective delivery of minimally invasive medicine. As shown in Fig. 6C, Mukrime *et al.* reported a magnetically controlled bacterial microrobots for targeted localization and multistimuli-responsive drug release in three-dimensional (3D)

biological matrices.¹³⁵ Magnetic nanoparticles and nanoliposomes loaded with photothermal agents and chemotherapeutic molecules were integrated into *E. coli* with ~90% efficiency. Bacteria-based microrobots, outperforming previously reported *E. coli*-based microrobots, retained their original motility and navigated through biological matrices and colonized tumor spheroids under magnetic fields for on-demand release of the drug molecules by a near-infrared stimulus.

Diatoms, as the naturally porous silica structure, are promising substitutes for artificial mesoporous silica preparation. In Fig. 6D, Li *et al.* proposed a biohybrid magnetic microrobot based on *Thalassiosira weissflogii frustules* (TWFs) as a cargo packet for targeted drug delivery using a simple preparation method.¹³⁰ They could be precisely controlled to follow specific trajectories or to move as swarms. The cooperation of the two motion modes of biohybrid microrobots increased microrobots' environmental adaptability. Such microrobots utilize the porous structure of diatoms to load drugs and provide artificially modified magnetic layers to endow them with active and controllable properties, demonstrating great potential in targeted anticancer therapy.

4.1.2. Imaging. Efficient imaging agents can provide precise localization, effective early diagnosis and treatment monitoring for precise treatment, and provide considerable guidance for intelligent therapy, especially cancer treatment.¹⁴⁴ Currently, several biomedical imaging techniques, such as fluorescence



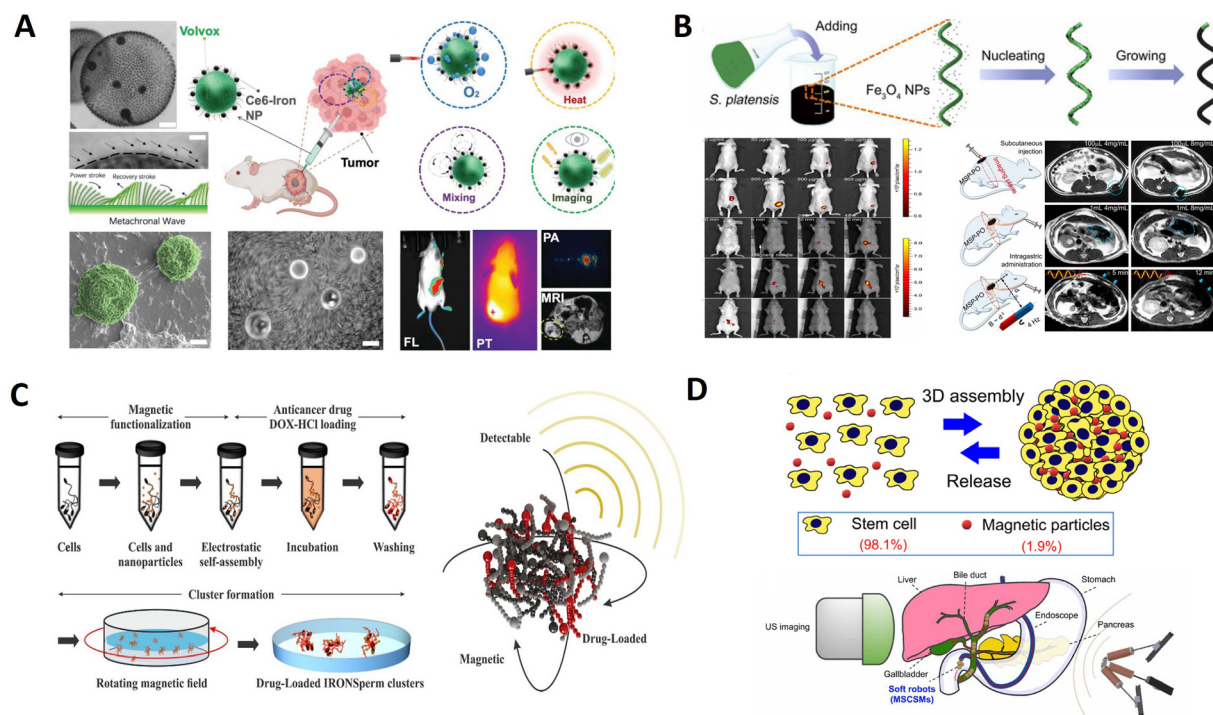


Fig. 7 Biotemplate-based micro/nanorobots for imaging. (A) Volvox microalgae-based robots for multimode precision imaging and therapy. Reprinted with permission from ref. 131. Copyright 2022 Wiley-VCH. (B) Multifunctional biohybrid magnetite microrobots for imaging-guided therapy. Reprinted with permission from ref. 119. Copyright 2017 AAAS. (C) Drug-loaded IRONSperm clusters: modeling, wireless actuation, and ultrasound imaging. Reprinted with permission from ref. 101. Copyright 2022 IOP Publishing. (D) Endoscopy-assisted magnetic navigation of biohybrid soft microrobots with rapid endoluminal delivery and imaging. Reprinted with permission from ref. 153. Copyright 2021 AAAS.

imaging (FLI),¹⁴⁵ photothermal imaging (PTI),¹⁴⁶ photoacoustic imaging (PAI),¹⁴⁷ magnetic resonance imaging (MRI),¹⁴⁸ computer tomography (CT),¹⁴⁹ and positron emission tomography (PET),¹⁵⁰ have been developed, that have improved the spatial resolution of cancer imaging. With the development of nanotechnology, biotemplates with unique properties have recently become an exciting prospect for accurate cancer imaging. Visual positioning of micro/nanorobots based on a biotemplate is crucial for achieving motion, path planning, and autonomous navigation based on visual feedback.¹⁵¹ To this end, various biotemplate-based micro/nanorobots with imaging functional have been applied to visualization. The following sections will discuss the progress of integrating imaging strategies with the motion-tacking of biotemplate-based micro/nanorobots.

The selection of unique motile microorganisms that combine the advantages of locomotion with imaging materials, such as imaging agents and photothermal agents, could assist in addressing the challenges of cancer regions. As shown in Fig. 7A, Wang *et al.* developed an all-in-one self-propelled volvox-based multifunctional robot, Volbot, with built-in fluid mixing capabilities, multimode imaging, and photosynthesis-mediated *in situ* oxygen generation that can potentially relieve hypoxia.¹³¹ Volbots can follow a pre-specified route and directionality under the control of a magnetic field. Red-light irradiation ($\lambda = 650$ nm) can enhance the Volbot's locomotive behavior, enhance the mixing of biofluids, and modulate the oxygen production to improve the efficacy of photodynamic

therapy. Moreover, Volbots can absorb near-infrared radiation to produce localized hyperthermia and offer imaging capabilities for treating tumors. The use of volvox as the engine of the robot provides unique advantages over other strategies that employ microorganisms, as volvox *in situ* generates oxygen; self-fluoresces for use in multimodal imaging; has autonomous phototaxis navigation capability; enables built-in fluid pumping/mixing generated by the synchronized beating of its flagella; and facilitates localized photodynamic, as well as photothermal therapy.

The innate properties of microalgae allowed *in vivo* fluorescence imaging and remote diagnostic sensing without any surface modification. As shown in Fig. 7B, Yan *et al.* reported a type of biotemplate-based magnetite microrobot that is imageable, biodegradable, and selectively cytotoxic to cancer cells.¹¹⁹ This fabricated biotemplate-based magnetite microrobot can perform robust navigation in various biofluids and be noninvasively tracked by auto-FL/MR imaging in either superficial tissues or deep organs. Furthermore, it exhibits desirable biodegradability, remote diagnostic sensing ability, and anti-cancer potential. With its *in vivo* monitoring *via* bimodal imaging features, tunable degradation *via* dip-coating control, and inclusiveness of functionality extension/drug loading *via* surface modification, this biotemplate-based microagent represents a microbiobotic vehicle with a high potential for imaging-guided therapy.

Ultrasound imaging is a potential option for noninvasive localization and has been established as a standard clinical



diagnostic tool. It is radiation-free and provides real-time imaging, allowing microrobot tracking.¹⁵² As shown in Fig. 7C, Middelhoek *et al.* fabricated drug-loaded biotemplate-based clusters and understood their characteristics to enable wireless rolling locomotion and ultrasound imaging simultaneously.¹⁰¹ Nanoparticle-coated sperm cells can be electrostatically and magnetically entangled in dense clusters of up to 120 cells to obtain biotemplate-based clusters of microrobots. This aggregation of microrobots enables them to roll collectively in a predictable way in response to an external rotating magnetic field. It enhances ultrasound detectability and drug loading capacity compared to individual microrobots. The favorable features of biotemplate-based microrobot clusters emphasize the importance of investigating and developing collective microrobots and their potential for *in vivo* imaging.

Imaging functions can also be achieved through the self-assembly of cells. As displayed in Fig. 7D, Wang *et al.* developed soft and resilient magnetic stem cell spheroid microrobots (MSCSMs) using the three-dimensional (3D) self-assembly of stem cells doped with a low dose of magnetic particles.¹⁵³ An integrated robotic platform was developed to deliver the microrobots into the deep and narrow spaces inside the body, termed endoscopy-assisted magnetic actuation with a dual imaging system (EMADIS). In EMADIS, the endoscope offers an “express lane” for the MSCSMs to avoid direct contact with the complex fluidic environments and facilitates rapid passage through multiple biological barriers in organs and tissues. The magnetic field actuation guides the high-precision delivery of the MSCSMs to the targeted position after endoscopic deployment. Moreover, the endoscopic view and ultrasound imaging track the entire process. In this way, EMADIS enables the rapid and high-precision delivery of soft microrobots in real time for the targeted therapeutic intervention of hard-to-reach regions, which are inaccessible and even invisible by means of conventional endoscopes and medical robots.

4.1.3. Biosensing. Biosensors are ubiquitous in various disciplines, such as biochemical, electrochemical, agricultural,

and biomedical fields. They can recognize a biological event on a transducing device using a signal proportional to the analyte concentration to quantify a biological or biochemical response.¹⁵⁴ Different from passive materials, active biotemplate-based micro/nanorobots have shown promising prospects in biosensing due to their unique active motion properties and easy functionalization. Especially, the movement of biotemplate-based micro/nanorobots with various receptors can realize “on the fly” capturing analytical targets.¹⁵⁵ Next, some biotemplate-based micro/nanorobots for advanced biosensor research are introduced.

Spores are produced by a wide range of plant or fungi species, and their unique and intricate 3D architecture can protect sensitive genetic materials from extreme environmental conditions. Zhang *et al.* developed highly efficient fluorescent magnetic pore-based microrobots for detecting toxins secreted by *Clostridium difficile* (*C. diff*) bacteria (Fig. 8A).¹³⁹ These microrobots were rapidly synthesized inexpensively by stepwise encapsulation and functionalizing the porous natural spores. Incorporating superior magnetic Fe₃O₄ nanoparticles facilitates the magnetic actuation of the droplet-like microstructure and even similar counterparts feasible in different media, showing continuous and efficient propulsion trajectories. Such a continuous and efficient movement greatly increases the diffusion and mass transport of the detected substance, thus facilitating higher detecting ability than static counterparts. Motion-based detection through tracking the emerging micro/nanorobots has shown great potential in chemo- and biosensing due to accelerated “chemistry on the move.”

Red blood cells (RBCs) can be trapped and manipulated by optical forces, which benefits their function as living biosensors and micromotors.¹⁵⁶ As shown in Fig. 8B, Li *et al.* constructed a living biosensor and micromotor from *in vivo* RBCs for pH sensing and particle transport applications.¹⁵⁷ The light propagation mode of the RBC waveguide was sensitive to the surroundings. After sensing pH, the formed RBC waveguide could continuously rotate as a micromotor because of the optical torque generated by the asymmetrical distributions of



Fig. 8 Biotemplate-based micro/nanorobots for biosensing. (A) Real-time tracking of fluorescent magnetic spore-based microrobots for remote detection of *C. diff* toxins. Reprinted with permission from ref. 139. Copyright 2020 Springer Nature. (B) Red-blood-cell waveguide as a living biosensor and micromotor. Reprinted with permission from ref. 157. Copyright 2019 Wiley-VCH.



the coherent output light from the fiber probes, enabling controllable microparticle delivery in the blood. In order to extend its potential application, the RBC waveguide was also successfully assembled and operated in zebrafish blood vessels. These phenomena inspired us to directly incorporate *in vivo* cells into a single device with sensing and actuation capabilities.

4.1.4. Anti-biological infection. Clinically, due to the complex interaction between pathogens and hosts, the combination of viruses and bacteria causes a very high mortality rate, posing a severe threat to human health worldwide.^{158,159} There are many treatments, but their effects are often not specific because anti-inflammatory drugs are not delivered to specific sites. Thus, developing active dosing of anti-inflammatory drug delivery systems to achieve the effects of local release of anti-inflammatory drugs and auxiliary sterilization has become an important research direction for anti-infection in recent years. Based on the active propulsion characteristics of micro/nanorobots and the excellent biocompatibility of biomaterials, some bio-based micro/nanorobots have been developed for anti-biological inflammation and will be described in the following chapters.

The natural sea urchin-like sunflower pollen (with sharp edges) is converted into capsule micro robots for loading drugs to remove biofilms. Sun *et al.* designed a magnetic urchin-like capsule robot loaded with magnetic liquid metal droplets (MUCR@MLMD) by using natural sunflower pollen as a biotemplate carrier for eradicating complex mixtures of a bacterial biofilm within biliary stents collected from patients (Fig. 9A).⁹³ Driven by an external magnetic field, the MUCR@MLMD

swarms actively target biofilm structures, first physically disrupting the extracellular polymeric substance barrier using the inherited microspikes of MUCRs. The carried MLMDs are then released to penetrate the biofilm and use their sharp edges to kill a variety of embedded bacterial cells, ultimately achieving synergistic biofilm eradication without the development of drug resistance. The robots benefit from the natural spikes of sunflower pollen that can be used to treat biofilms, physically destroying the protective effect and mechanical stability of EPS. Besides, Carmen *et al.* present a new concept using aqua sperm micromotors to destroy bacterial biofilms.¹⁰⁵ They use aqua sperm from North African catfish-as microrobots with head sized $\approx 1.5 \mu\text{m}$ compared with, for example, bovine sperm of head sizes $\approx 10 \mu\text{m}$. Their small size allows them to penetrate and disturb the biofilm matrix. Moreover, research has proved that their ultra-fast speed is efficient at destroying biofilms in a short time (displayed in Fig. 9B).

Furthermore, pathogenic bacteria in deep tissue penetration can also be used as a multifunctional magnetic bio-microswimmer. By mimicking a corkscrew motion of the *Escherichia coli*, such micro/nanoswimmers can perform remotely controlled navigation in a wide range of complex environments filled with biofluidic media. As shown in Fig. 9C, Xie *et al.* developed a multifunctional magnetic microswimmer based on *Spirulina* to treat pathogenic bacterial infection.¹¹³ The microswimmer (PDA-MSP) consists of a magnetized *Spirulina* (MSP) matrix and a polydopamine (PDA) surface, which not only preserve the desirable properties of the original MSP but also endowed it with additional functions aimed at the



Fig. 9 Biotemplate-based micro/nanorobots for anti-biological infection. (A) Magnetic microswarm and fluoroscopy-guided platform for biofilm eradication in biliary stents. Reprinted with permission from ref. 93. Copyright 2022 Wiley-VCH. (B) Swarming aqua sperm micromotors for active bacterial biofilms removal in confined spaces. Reprinted with permission from ref. 105. Copyright 2021 Wiley-VCH. (C) Photoacoustic imaging-trackable magnetic microswimmers for pathogenic bacterial infection treatment. Reprinted with permission from ref. 113. Copyright 2020 American Chemical Society.

treatment of pathogenic bacterial infection. In this study, the developed microswimmer based on a spiral shape can undergo motion *in vivo*, and can be used for PDA-enabled PA imaging, off-on fluorescence diagnosis, as well as photothermal therapy for the theranostics of pathogenic MDR KP infection.

4.1.5. Antibacterial. Diseases caused by bacterial infections are once again recognized as a severe global threat to human health due to the emergence and rapid spread of bacterial resistance to available antibiotics and the limited progress in discovering and developing new effective anti-bacterial agents.¹⁵⁸ The preparation of composite micro/nanorobots with special structures and properties by the bio-template method is one of the research hotspots in the field of materials science today. Its advantage lies in the spatial limitation and regulatory role of biological templates that can achieve control over composite materials' surface morphology and structure, not only to obtain composite materials with specific surface morphology but also to achieve an effective composite between nanoscale particles and large-scale biotemplates. In particular, using micro/nanorobots with active propulsion as cargo delivery systems provides an alternative strategy for transporting therapeutic drugs to desired locations that are difficult to reach using traditional strategies. Based on this, a series of biotemplate-based micro/nanorobots for antibacterial application have been developed.

Helical microswimmers can be effectively actuated and can perform controlled locomotion in various fluids; therefore,

they can envision precise micromanipulation and efficient environmental purification in low-strength rotating magnetic fields. As displayed in Fig. 10A, Zheng *et al.* reported a core-shell-structured porous hollow helical microswimmer possessing an inner carbon core of porous surfaces and an outer magnetic shell aggregated by mesoporous spindle-like magnetite nanoparticles (NPs).¹¹⁴ This microswimmer is fabricated using a high-yield template process based on helical *S. platensis*. Attributed to the existing magnetite NPs of the outer shell, the obtained swimmers have superparamagnetic nature and high magnetic saturation; therefore, they can perform magnetically actuated corkscrew motions under low-strength rotating magnetic fields. More importantly, such swimmers inherit good photothermal attributes and high specific surface area from their magnetite-carbon composition and porous hollow structures, respectively, which can be used for photothermal antibacterial treatment, biological detoxification, and targeted delivery.

To avoid harmful NIR light and fully use solar energy, using high efficiency visible light inactivating bacteria *via* the use of natural biotemplates as raw materials is an important target. As shown in Fig. 10B, Xu *et al.* developed a facile and cost-effective biotemplate method to fabricate a visible light stimulated magnetic microrobot with enhanced photocatalytic antibacterial performances.¹⁰⁶ Fe_3O_4 nanoparticles (NPs) and BiOCl nanosheets (NSs) were deposited on bio-templates in sequence to form $\text{Ch.}@Fe_3O_4@BiOCl$ (CFB) microrobots. The composite

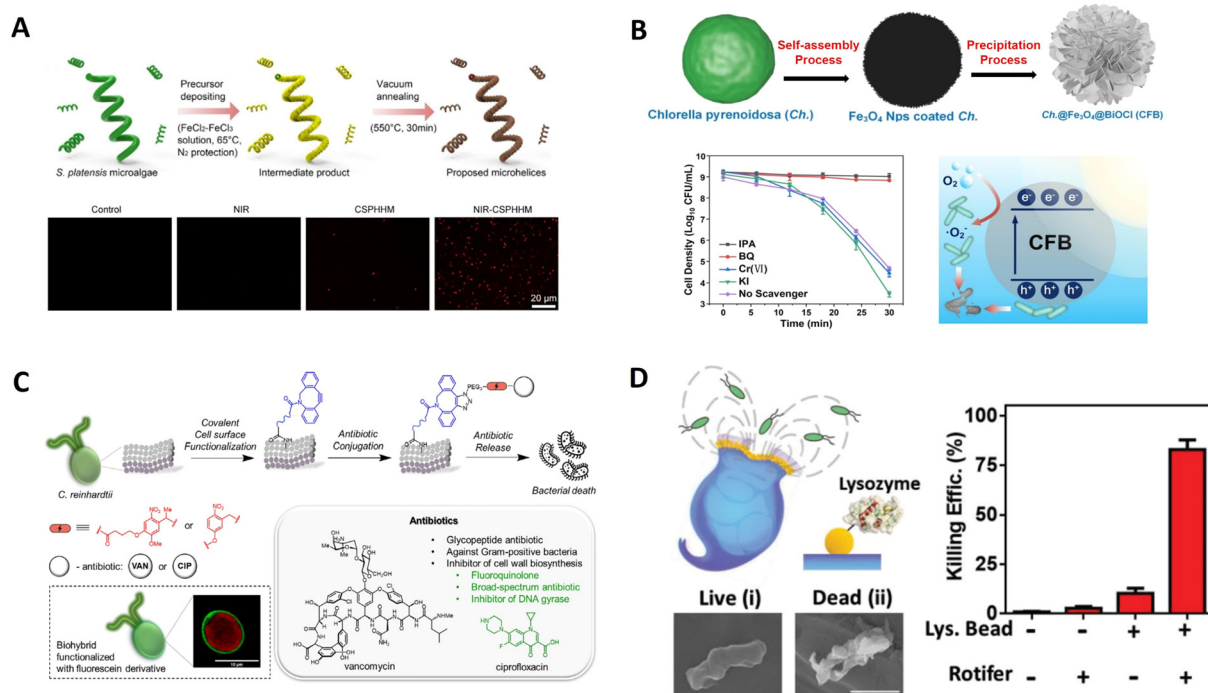


Fig. 10 Biotemplate-based micro/nanorobots for antibacterial. (A) Spirulina-templated porous hollow carbon@magnetite core-shell microswimmers. Reprinted with permission from ref. 114. Copyright 2021 Elsevier. (B) Biohybrid magnetic microrobots for enhanced *E. coli* inactivation under visible light irradiation. Reprinted with permission from ref. 106. Copyright 2022 Elsevier. (C) Biohybrid microswimmers against bacterial infections from ref. 122. Copyright 2021 Elsevier. (D) Rotibot: Use of rotifers as self-propelling biohybrid microcleaners. Reprinted with permission from ref. 160. Copyright 2019 Wiley-VCH.

structure and abundant natural photosensitizers in the biotemplates endowed them with rapid photocatalytic capability under visible light irradiation, leading to excellent photocatalytic inactivation of *E. coli*. Under collective rolling mode with enhanced fluidic interactions, the bacterial inactivation rate could also be increased over 30%. Such an excellent performance can be ascribed to the composite microstructure, the abundant natural photosensitizers in the biotemplate, and enhanced fluidic interactions under magnetic actuation.

Bacteria-based biotemplate-based systems face multiple issues, including potential pathogenicity or immunogenicity, rapid growth rate, and potential to develop antibiotic resistance.²⁴ *C. reinhardtii* is known as a phototactic green microalga, and swims steadily towards or away from the light stimulus due to optical receptors. Shchelikh *et al.* reported a strategy for biohybrid microswimmers, which features the covalent attachment of antibiotics with a photo-cleavable linker to the algae *C. reinhardtii* via two synthetic steps (Fig. 10C).¹²² This surface engineering does not rely on genetic manipulations, proceeds with high efficiency, and retains the viability or phototaxis of microalgae. This study demonstrated the application of biotemplate-based microswimmers for caging and controlled release of different types of antibiotics that can expand their use against various bacterial infections. The microswimmers could be guided to a particular region to precisely release their antibacterial cargo.

Rotifers control fluid flow by beating their cilia bands for efficient locomotion and feeding. In addition, the robots were evaluated initially as potential antibacterial microcleaners. Based on these, Soto *et al.* engineered a new biotemplate-based microswimmer featuring antibacterial properties (Fig. 10D).¹⁶⁰ The microbeads were functionalized with lysozyme enzymes capable of cleaving glycosidic bonds of peptidoglycans present in the cell walls of different bacteria. The high fluid flow toward the mouth, generated by the strokes of rotifer cilia bands, forces an extremely efficient transport of the contaminated sample over the active surfaces of the functionalized microbeads. The reactive particles confined around the rotifer's lip are thus exposed to a high flow rate of the pollutant solution, resulting in dramatically accelerated antibacterial processes without external mixing or harmful fuels. In this, the rotifer can serve as an extremely efficient self-propulsion engine of the biohybrid microrobot and integrate capabilities that respond to environmental signals and maneuver effectively in their environment.

4.1.6. Capture of organisms. A micro/nanorobot with self-propelled properties and navigating in complex fluidic environments allows localization, pick-up, and delivery of microscopic and nanoscopic objects.¹⁶¹ All these capabilities have made the micro/nanorobot an ideal candidate to serve as a tiny vehicle for capture and targeted drug delivery. In this regard, some special biotemplate-based microswimmers composed of a living microswimmer integrated with artificial structures are designed as practical tools for active capture of organisms and cargo delivery. Next, we will elaborate with some concrete examples.

The natural spiral structure endows micro/nanorobots with excellent motion performance by converting rotational motion to translational motion. In our previous study, we developed a

biotemplate-based microswimmer for efficiently capturing and transporting cancer cells as well as killing the cells under light irradiation.⁸⁷ The spiral vessels isolated from banana leaves were used as biological templates, where nickel layers with magnetic properties and Fe³⁺-TA (tannic acid, TA) films with pH-dependent degradation capabilities were modified on their surfaces by simple chemical reactions in solution at room temperature (Fig. 11A). Due to the specific chemical interaction between the microswimmers and the surface of cancer cells, the microswimmers can precisely capture and transport these cancer cells in the presence of a magnetic field. Using biotemplates with spiral structures in this way provides a new approach to preparing multifunctional micro/nanorobots.

Pollen grains have a large inner cavity for encapsulating genetic materials, multiscale channels, and numerous spikes on the outer shell or extine. Based on this, Song *et al.* successfully developed a light-controlled micromotor with efficient motion and loading capacity based on sunflower pollen grains (Fig. 11B).⁹⁴ In their experiments, as a live cargo model, yeast cells were captured and located in the gap of the micromotors' spikes. The room between the neighboring spikes was like a grip, which firmly grasped the cells with the increased contact surface. Therefore, micromotors provide a larger surface contact area to increase the binding odds between micromotors and cells, which eventually benefits the capture efficiency. In addition, Song *et al.* developed a light-controlled microrobot for capturing and gathering bacteria based on photothermal effects (Fig. 11C).⁹⁵ The sterilization microbots were fabricated from carbonized sunflower pollen grains with a polydopamine coating. A bacterial capture molecule, vancomycin, is grafted onto the outer surface of polydopamine. Under the focused laser, the microbot can show positive phototactic motion and bubble-induced gathering powered by the photothermal-induced Marangoni effect for efficient capture and aggregation of the targeted bacteria. Such microbots could provide a new proof-of-concept perspective on capturing bacteria and sterilization applications.

4.1.7. Cancer treatment. Cancer has been one of the fatal diseases threatening human health in recent decades.¹⁶² Recent studies have shown that preparing multifunctional micro/nanorobots with active control and functionalization at the microscale for *in vivo* cancer therapy is promising. Biotemplates are receiving increasing attention as raw materials for manufacturing micro/nanorobots. Nature provides unique biotemplates with various structures that can be used to manufacture functional micro/nanorobots for different applications.¹⁸ Compared to existing manufacturing methods, biological hybridization methods based on natural materials can eliminate complex processes, showing the advantages of cost-effectiveness and simplicity. At this time, a series of functional biotemplate-based micro/nanorobots for cancer therapy emerged due to their active propulsion characteristics and good biocompatibility.

Among the pollen grains, chrysanthemum pollen grains possess excellent morphological characteristics after sequential treatment, like spiny protrusion, hollow cavities, and porous





Fig. 11 Bi-template-based micro/nanorobots for organisms. (A) Bifunctional biohybrid magnetically propelled microswimmer. Reprinted with permission from ref. 87. Copyright 2022 Elsevier. (B) Light-controlled spiky micromotors for efficient capture and transport of targets from ref. 94. Copyright 2022 Elsevier. (C) Light-controlled microbots gathering as a sterilization platform for highly efficient capturing, concentrating and killing targeted bacteria. Reprinted with permission from ref. 95. Copyright 2022 Elsevier.

surface structures. These attractive features could be fully utilized for specific functions, making them an attractive platform to provide comprehensive therapeutic strategies for biomedical applications. Chrysanthemum pollen grains possessing a large internal cavity were used for drug encapsulation and the ordered burr-like microspikes around the surface could be utilized for physical assassination to kill tumor cells. Utilizing natural morphological characteristics, Liu *et al.* developed chrysanthemum pollen-derived bi-template-based magnetic microrobots for synergistic tumor therapy by combining magnetically controlled physical assassination and active drug delivery.⁸² As shown in Fig. 12A, the microrobots could be actively steered for targeted cell delivery and tissue regeneration under a magnetic field. This bi-template-based microrobot provides a typical example of utilizing natural morphologies to develop multifunctional active matter at the microscale for the next generation of active therapeutics.

Microalgae have a high capacity of light absorption (*e.g.*, UV light) because of their various chromophores and have antioxidant and anti-inflammatory properties. They have been used for other types of phototherapies to treat skin diseases such as cancer and inflammatory diseases. Considering all the factors mentioned above, as shown in Fig. 12B, Wang *et al.* proposed a strategy that uses biomaterial *Sp.* as a scaffold to fabricate magnetic microrobots. They can load anticancer drugs and photothermal agents to achieve synergistic and enhanced therapeutic efficacy.⁷⁰ The microrobots can be degraded under NIR irradiation and exhibit pH- and NIR-triggered drug release to realize cancer therapy. This work provides an integrated route for fabricating multifunctional microrobots with high swimming speed, precise directional guidance, ultrahigh drug

loading efficiency, and efficient photothermal conversion ability toward targeted delivery applications and synergistic chemophototherapy in a single platform.

In addition, bacteria-based microrobots can offer valuable intrinsic characteristics of bacterial microorganisms, such as self-sensing, self-propulsion, fluorescence, and chemotaxis toward tumor sites. *Magnetococcus marinus* strain, *magnetospirillum magneticum* (AMB-1), is a candidate for preparing functionalized micro/nanorobots for tumor therapy because magnetosomes inside the body are susceptible to external magnetic fields and can be autonomously manipulated to the tumor site. Xing *et al.* reported a bi-template-based microrobot (Fig. 12C) composed of motile AMB-1 and light-triggered indocyanine green nanoparticles (INPs).⁷⁸ The INPs, as a hitchhiker circulates in the blood, are transported by magnetotaxis bacteria AMB-1 with magneto-anaerobic behavior, and then enriched in tumors for subsequently ablating the tumors by photothermal therapy under NIR laser irradiation. AI microrobots based on autonomous flagellum propulsion of AMB-1 can realize controlled navigation, focal localization, deep penetration, and tumor colonization *in vivo*.

Spermatozoa are highly efficient micromotors perfectly adapted to traveling up the female reproductive system. Indeed, bovine sperm-based micromotors have shown the potential to carry drugs for gynecological cancer treatment.¹⁶³ As shown in Fig. 12D, Xu *et al.* presented a fully functional drug delivery system based on human sperm.¹⁰³ In order to establish a robust pipeline for anticancer drug loading (DOX, model drug) in human sperm, they investigated the DOX loading mechanism and integrated the system into a versatile enhancement



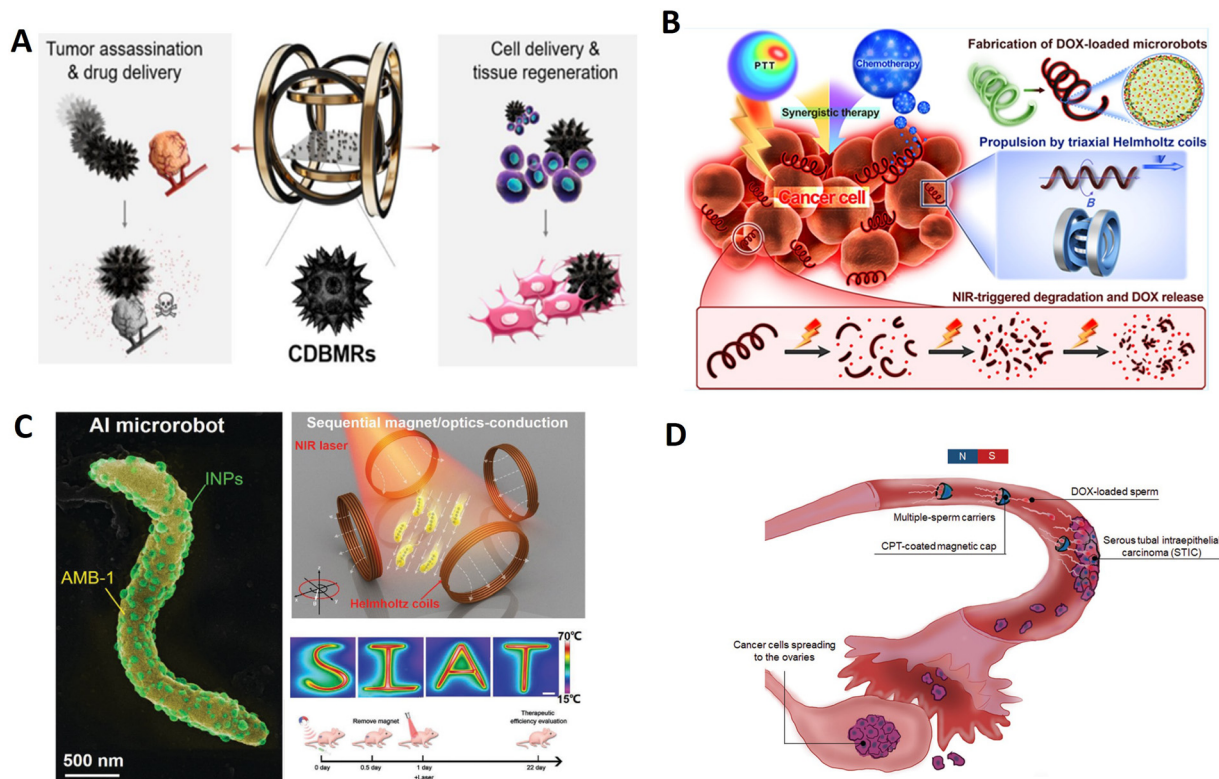


Fig. 12 Biotemplate-based micro/nanorobots for cancer treatment. (A) Biohybrid magnetic microrobots for tumor assassination and active tissue regeneration. Reprinted with permission from ref. 82. Copyright 2022 American Chemical Society. (B) Facile fabrication of magnetic microrobots based on spirulina templates for targeted delivery and synergistic chemo-photothermal therapy. Reprinted with permission from ref. 70. Copyright 2019 American Chemical Society. (C) Sequential magneto-actuated and optics-triggered biomicrorobots for targeted cancer therapy. Reprinted with permission from ref. 78. Copyright 2021 Wiley-VCH. (D) Human sperm-bots for patient-representative 3D ovarian cancer cell treatment. Reprinted with permission from ref. 103. Copyright 2020 Royal Society of Chemistry.

platform suitable for targeting early ovarian cancer lesions. The study of free-swimming sperm technologies will become more critical in the diagnostic and therapeutic field.

4.1.8. Other biological applications. Functional biotemplate-based micro/nanomotors are a potential development direction of micro/nanorobots. Biotemplate-based micro/nanomotors have good biocompatibility and loading. Combined with outfield driving or self-directional movement, they have played an essential role in drug targeting, imaging, cancer treatment, and other aspects of the human body. Therefore, among many future applications of biotemplate-based micro/nanorobots, applications in the biomedical field will be up-and-coming. Simultaneously, with the continuous deepening and development of research, micro/nanorobots will gradually play a more significant role in biological applications. Next, we will introduce more biological micro/nanorobot applications in biomedicine.

Recently, biotemplate-based micro/nanorobot technology has been applied to improve plant cell growth, aid in the differentiation process, or in their reproduction to produce new plants. Huska *et al.* developed a new methodology to obtain plant cell motors by translocation of ferromagnetic materials (Fe_3O_4) inside tomato-biobots during their callus growth (Fig. 13A).⁸⁹ In this study, they have demonstrated that

the translocation of Fe_3O_4 did not affect the viability of plant biotemplate-based robots. Developed tomato-biobots can drive by a transversal rotating magnetic field. In addition, the proposed methodology produces tomato-biobots that can load, store, and deliver biomolecules and thus significantly improve health, growth, and dividing plant callus cells. In this way, they have demonstrated that they can generate tomato cell clones from plant biotemplate-based robots. The research is still in the beginning stage; however, it is highly promising and offers unexpected opportunities of great dimensions that could revolutionize the entire biotechnology world.

C. reinhardtii is a biflagellate unicellular freshwater green microalga. Due to their ideal size, abundance, motility, and biocompatibility, *C. reinhardtii* cells are excellent natural candidates as living rotary micro motors to actuate microflows precisely. Pan *et al.* reported optical trapping-driven biomicromotor tweezers by using living *C. reinhardtii* alone for noninvasive delivery of bio-cargos, including microparticles, cells, and drugs further for precise cancer cell therapy (Fig. 13B).¹²⁴ By actuating a localized flow field around different targeted bio-cargos, two optically trapped rotating CR cells potentially act as micromotor tweezers for noncontact capture and transport of bio-cargos along arbitrary trajectories in bio-microenvironments in a noninvasive, flexible, and biocompatible manner.



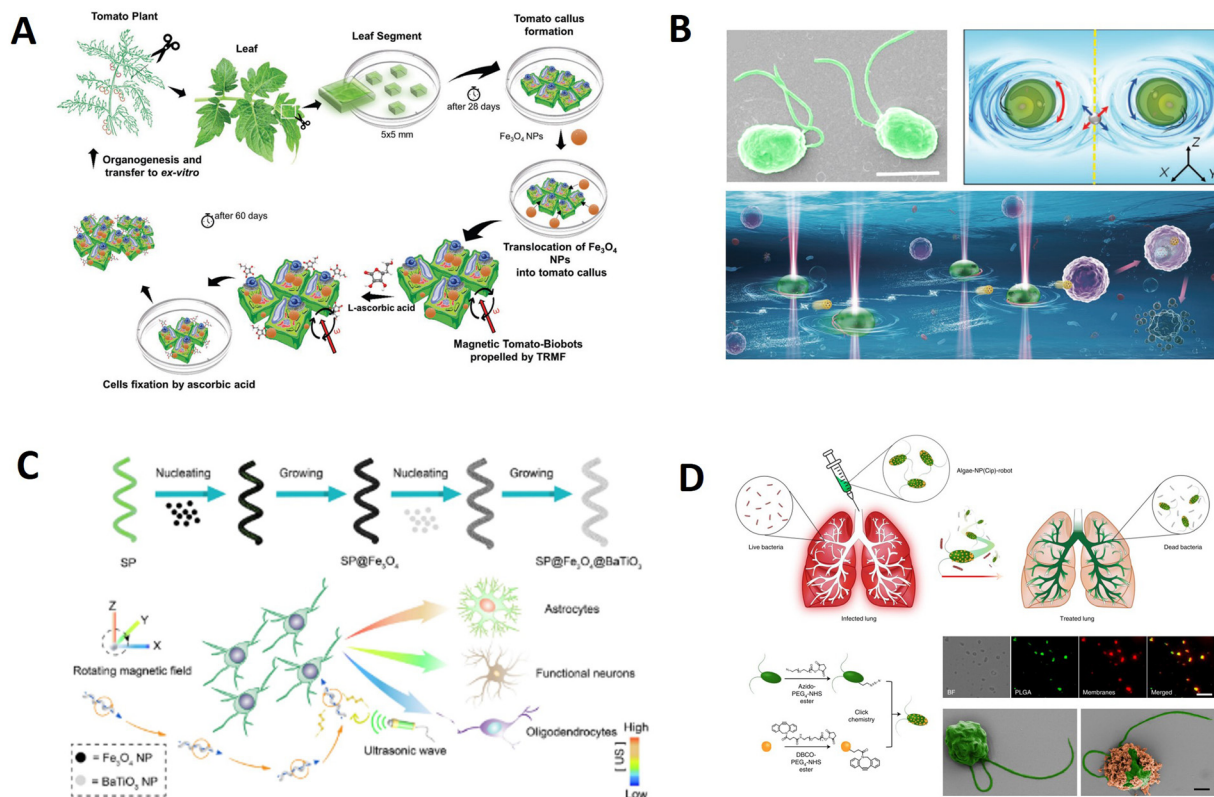


Fig. 13 Biotemplate-based micro/nanorobots for biological applications. (A) Magnetic biohybrid robots as efficient drug carrier to generate plant cell clones. Reprinted with permission from ref. 89. Copyright 2022 Wiley-VCH. (B) Bio-micromotor tweezers for noninvasive bio-cargo delivery and precise therapy. Reprinted with permission from ref. 124. Copyright 2022 Wiley-VCH. (C) Controlling the neural stem cell fate with biohybrid piezoelectrical magnetite micromotors. Reprinted with permission from ref. 117. Copyright 2021 American Chemical Society. (D) Nanoparticle-modified microrobots for *in vivo* antibiotic delivery to treat acute bacterial pneumonia. Reprinted with permission from ref. 121. Copyright 2022 Nature Research.

Such bio-micromotor tweezers depend on the motion of *C. reinhardtii* and provide great potential for different biomedical applications such as targeted drug/cell delivery, drug testing, accurate diagnosis, and precise therapy.

Inducing neural stem cells to differentiate and replace degenerated functional neurons represents the most promising approach for degenerative neural diseases, including Parkinson's disease, Alzheimer's disease, *etc.* While diverse strategies have been proposed in recent years, most of these are hindered due to uncontrollable cell fate and device invasiveness. Thus, Liu *et al.* reported a minimally invasive micromotor platform with biodegradable helical *S. platensis* as the framework and superparamagnetic Fe_3O_4 nanoparticles/piezoelectric BaTiO_3 nanoparticles as the built-in function units (Fig. 13C).¹¹⁷ With a low-strength rotational magnetic field, this integrated micromotor system can precisely navigate in biofluids and achieve single-neural stem cell targeting, which is attributable to helical structures and magnetic layers endowed with directional motion, enabling it to become a system capable of controlling the differentiation fate of the neural stem cells *in situ* in a simple, wireless, and minimally invasive way.

Neutrophil membrane-coated NPs are used because of their unique cell-mimicking properties, including shielding payloads from biological environments, reducing immune clearance and

enabling specific binding with target pathogens. Natural algae can be combined with the engineering versatility of biomimetic NPs to yield a hybrid microrobot platform capable of active drug delivery. In Zhang *et al.*'s design, they create a biotemplate-based microrobot consisting of *C. reinhardtii* microalgae modified with neutrophil membrane-coated and drug-loaded polymeric nanoparticles (denoted as 'algae-NP-robot') for the *in vivo* treatment of lung infection (Fig. 13D).¹⁶⁴ In a mouse model of acute *Pseudomonas aeruginosa* pneumonia, the microrobots effectively reduced the bacterial burden and substantially lessened animal mortality with negligible toxicity. Overall, these findings highlight the attractive functions of algae-nanoparticle hybrid microrobots for the active *in vivo* delivery of therapeutics to the lungs in intensive care unit settings.

4.2. Environmental applications

Rapid industrialization generates a large number of chemical wastes, such as dyes, oils, pesticides, heavy metal ions, and others. These harmful organic substances accumulated in our surroundings threaten human health. However, conventional chemical detoxification technology typically needs prolonged operation time and/or mechanical stirring, and is low-efficient for water treatment.¹⁶⁵ Due to their autonomous motion properties, the burgeoning micro/nanorobots can accelerate the



process by enhancing contact with the treatment solution.⁸⁷ Unlike conventional processes, self-propulsion micro/nanorobots are promising in fast and advanced water treatments. The customizable surface of micro/nanorobots can be functionalized with catalysts and adsorbent functions for the catalytic degradation and adsorptive removal processes.¹⁶⁶ By reasonable structure design and surface functionalization, micro/nanorobots have been developed as powerful “on-the-fly” cleaning platforms for removing organic, inorganic, and biological pollutants.¹⁶⁷ Natural biotemplates are renewable plants with special structures and can be easily obtained at a low price, enabling the mass preparation of intelligent micro/nanorobots at an inexpensive cost. Thus, a series of micro/nanorobots with an excellent capacity based on biotemplates as templates were developed.

4.2.1. Adsorbed metal ions. Many heavy metals, such as copper, nickel, cobalt, zinc, arsenic, mercury, cadmium, chromium, lead, and so on, prove cumulatively toxic to living organisms and long biological half-lives.¹⁶⁸ Over the past centuries, the gradually increasing levels of metals in water solutions have reached an alarming value, thus putting forward an urgent need for developing novel materials and technologies to remove them in a green, efficient, and reusable fashion.¹⁶⁸ Benefiting from the excellent adsorption properties of biotemplates, living and dead microorganisms (such as bacteria, fungi, plant fiber, and algae) have remarkable uptake ability for metals, enabling them to sequester metal ions out of the

complex solution from the ppm to ppb level effectively and quickly.^{169,170} Considering their abundant sources, environmental friendliness, and vast adsorption capacity, integrating them with self-propelled micro/nanorobots is an ideal biosorption way to remove heavy metals in a green and effective manner.

Inspired by the natural kapok fiber with a unique hollow tubular structure containing cellulose and lignin, which could provide unbalanced force conditions in the motion of micro/nanomotors, Yang *et al.* reported a kapok fiber inspired functionalized Eu-MOF-based fluorescent micromotor. It is an active self-propelled micromachine for detecting, capturing, and removing Fe^{3+} from water (Fig. 14A).⁸³ This micromotor has the merits of high sensitivity, good selectivity, and high dynamic adsorption for Fe^{3+} . Based on this, it can be extended to detecting and removing other target ions, boosting the preparation of fluorescent micromotors for environmental management. Compared with various conventionally static nanomaterials, self-propelled micromotors have greatly enhanced the efficiency of traditional operations due to the phenomena of active motion of matter and have been demonstrated to exhibit an extremely significant effect on the detection of various contaminants.

Lotus pollen grains, the sori of lotus, were selected as the biotemplate to prepare Janus micromotors due to their characteristic porous microporous morphology, acceptable cost, and ready availability.¹⁷¹ As seen in Fig. 14B, Han *et al.*

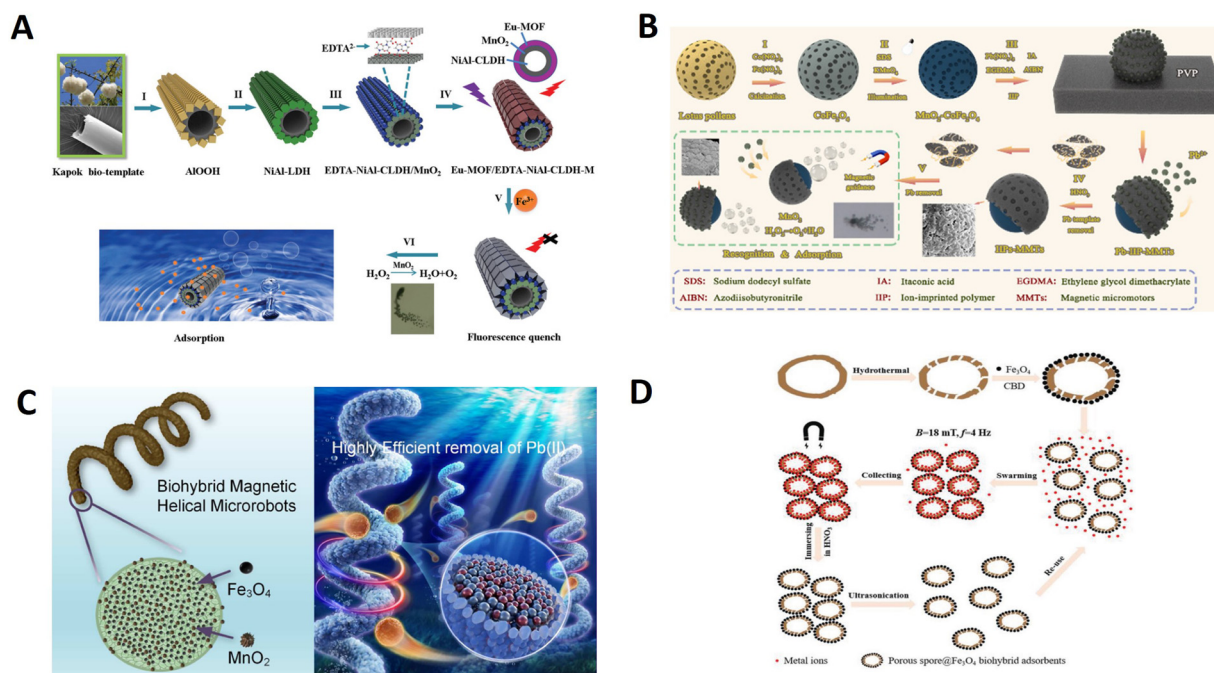


Fig. 14 Biotemplate-based micro/nanorobots for adsorbed metal ions. (A) An Eu-MOF/EDTA-NiAl-CLDH fluorescent micromotor for sensing and removal of Fe^{3+} from water. Reprinted with permission from ref. 83. Copyright 2019 Royal Society of Chemistry. (B) Ion-imprinted $\text{MnO}_2/\text{CoFe}_2\text{O}_4$ Janus magnetic micromotors synthesized by a lotus pollen template for highly selective recognition and capture of $\text{Pb}(\text{II})$ ions. Reprinted with permission from ref. 90. Copyright 2022 Royal Society of Chemistry. (C) Efficient removal of $\text{Pb}(\text{II})$ from aqueous systems using spirulina-based biohybrid magnetic helical microrobots. Reprinted with permission from ref. 111. Copyright 2021 American Chemical Society. (D) Enhanced removal of toxic heavy metals using swarming biohybrid adsorbents. Reprinted with permission from ref. 141. Copyright 2018 Wiley-VCH.



developed a novel Janus micromotor based on the combination of ion-imprinted recognition cavities and self-propelling motion for the sensitive recognition and removal of Pb(II) ions from water.⁹⁰ Ion-imprinted $\text{MnO}_2/\text{CoFe}_2\text{O}_4$ Janus micromotors inherit the porous structure of lotus pollen grains and reveal sensitive recognition and capture for Pb(II) ions and magnetic recovery capability. This study provides a new strategy for the highly selective removal of metal contaminating ions from water. Besides, microalgae have unique biological structures with plentiful active sites on the surface, such as hydroxyl and carboxyl groups, and both living and dead ones exhibit certain adsorption validity. Gong *et al.* presented Fe_3O_4 and MnO_2 -loaded biotemplate-based magnetic helical microrobots (BMHMs) based on *Spirulina* cells for Pb(II) removal (Fig. 14C).¹¹¹ The BMHMs could be magnetically actuated forward flexibly and perform continuous cork-screw spinning in swarm for intensive adsorption. Rapid and significant removal of Pb(II) was achieved using the swarming BMHMs. The adsorption capacity could reach 245.1 mg g^{-1} , higher than those of most of the reported MnO_2 -based adsorbents. The intriguing properties of the BMHMs enable them to be versatile platforms with significant potential in wastewater remediation.

Porous biotemplates are often used as adsorbents, such as *Ganoderma* spores. As shown in Fig. 14D, Zhang *et al.* developed a biotemplate-based adsorbent through *in situ* growing magnetic Fe_3O_4 nanoparticles on hydrothermally treated fungi spores.¹⁴¹ Such organic/inorganic porous spore@ Fe_3O_4 biotemplate-based adsorbents (PSFBAs) can effectively adsorb

and remove heavy metal ions due to porous structuring and high-adsorbing components. Once combined with a magnetically driven microrobotic technique, magnetic PSFBAs in controllably collective motion show enhanced adsorption capacity and shorter removal time for multiple heavy metal ions compared to nonmotile counterparts. Combining biological entities and swarming microrobotic techniques would provide a promising avenue for decontaminating pollutants in environmental remediation.

4.2.2. Removal of pollutants. Pollutants (such as rhodamine B, chlorpyrifos, oil, and microplastics) can cause severe soil, river, and groundwater pollution.^{172–175} Although several porous nano/microscale adsorbents have been developed to absorb pollutants, they are less efficient due to their passive motion property.^{97,176} Purifying them is also tedious work. In particular, biotemplate-based micro/nanorobots have shown a new dimension in motion-based decontamination processes and led to new “instant” remediation solutions, higher efficiency, shorter decontamination times, and potentially lower costs.

It is meaningful to achieve large-scale reproducible production of biotemplate-based micromotors for removing erythromycin (ERY) using a relatively facile procedure and acceptable cost. Li *et al.* used a facile bio-template route to synthesize a novel Pt-free temperature-responsive micromachine with fascinating recognition, capture and release capacities for erythromycin in water based on the integration of surface imprinted technology, the temperature-response of poly(*N*-isopropylacrylamide) (PNIPAM) hydrogels, and the autonomous motion



Fig. 15 Biotemplate-based micro/nanorobots for degrading pollutants. (A) Bioinspired Pt-free molecularly imprinted hydrogel-based magnetic Janus micromotors for temperature-responsive recognition and adsorption of erythromycin in water. Reprinted with permission from ref. 91. Copyright 2019 Elsevier. (B) Engineered magnetic plant biobots for nerve agent removal. Reprinted with permission from ref. 88. Copyright 2022 Nature Research. (C) Cooperative recyclable magnetic microsubmarines for oil and microplastics removal from water. Reprinted with permission from ref. 97. Copyright 2020 Elsevier. (D) Biotemplating of metal-organic framework nanocrystals for applications in small-scale robotics. Reprinted with permission from ref. 115. Copyright 2020 Wiley-VCH.

ability of a micromotor.⁹¹ The resulting Janus micromotor exhibited higher temperature-controlled recognition and adsorption capacities than most reported erythromycin-imprinted materials but also revealed high trajectory control ability and easy recovery by an external magnetic field, showing great potential for biomedical and water purification applications (Fig. 15A). Besides, fabricating plant-derived biobots combined with plant tissue and ferromagnetic materials for decontamination is a new direction for biotemplate-based robots. Song *et al.* used tomato leaf-derived calli to fabricate plant robots, and their efficiency for chlorpyrifos removal was investigated.⁸⁸ The Fe₃O₄ NPs were transported through the cell growth media and then taken up into the plant tissue cells, imparting the plant biobot with magnetic function (Fig. 15B). The magnetic plant biobots demonstrated rapid and efficient removal of chlorpyrifos (approximately 80%).

The sunflower pollen grains (SPGs) have several remarkable structural features: large free volumes, multitudinous nanopores, and numerous nano spikes, which could make them attractive for water remediation. Sun *et al.* reported a “hedgehog” magnetic microsubmarine based on SPGs, which can simultaneously remove oil and microplastic pollutants.⁹⁷ As displayed in Fig. 15C, these hollow microsubmarines were fabricated on a large scale by sequentially treating the natural SPGs with acidolysis and sputtering. The hollow structure allows a double functionality: (i) like a submarine, propel under or above the water, depending on the fillings inside; (ii) oil pollutant storage. The microsubmarine can transport oil droplets 37 times larger than its volume and effectively adsorb floating oil *via* capillary action. And the fluid induced by the cooperative microsubmarines can remove the microplastics controllably in a noncontact method.

Furthermore, biotemplates can be extended to design MOF-based motors for various applications, from biomedicine to environmental remediation. Terzopoulou *et al.* presented a universal biotemplate-based methodology to fabricate 3D helical assemblies of MOF robotics.¹¹⁵ Specifically, *S. platensis* is used as a biotemplate on which multiple components comprising a magnetic chassis, a gelatin binder film, and a MOF nanocrystal coating are assembled (Fig. 15D). The robot is used to perform microrobotic targeted drug delivery in cancer cells due to high-precision 3D rotation and photocatalytic degradation of an organic pollutant in water. Such helical robots can be used as highly integrated magnetically driven microrobots with multiple functionalities.

4. Conclusion and outlook

Intelligent micro/nanorobots show good potential for applications in drug delivery, imaging, cancer therapy, environmental remediation and cargo handling due to their ability to convert external energy into motion under external magnetic fields. Utilizing natural materials as biotemplates to obtain intelligent micro/nanorobots is a new trend in recent years due to their elegant structures and abundant surface functional groups. Based on the characteristics of biotemplates, our review

introduced the advantages of natural materials as biotemplates, then systematically discussed the characteristics and preparation strategies of each type of intelligent micro/nanorobots, and finally summarized the applications of intelligent micro/nanorobots in different fields. Although great progress has been made in intelligent micro/nanorobots, there remain some shortcomings of current biotemplates. To further expand the potential of intelligent micro/nanorobots for applications, several challenges should be urgently considered and addressed. For example:

1. Source

Despite the relative abundance of biotemplates in nature, the sources of biotemplates for the preparation of specific structures are limited and are obtained by large-scale extraction from specific tissues or mass culture of microbial cells, which requires relevant extraction techniques, microbial culture techniques and the support of equipment. Therefore, it is necessary to develop an inexpensive and readily available biotemplate source.

2. Stability

The thermal stability of biotemplates is poor. When biotemplates are removed by heat treatment, high temperature can easily lead to the collapse of their porous structure and the loss of their micro/nanostructure, and they cannot play the role of templates or morphology inducers, which greatly limits their scope of use. Thus, it is important to choose the right biotemplates.

3. Lifetime

Considering that micro/nanorobots need to convert chemical fuels or diverse external energies to propulsion force for specific applications in versatile environments, it requires that micro/nanorobots possess long-term durability. Such micro/nanorobots can be used for recycling, which reduces resource and energy consumption and promotes sustainable development. Especially, live cells such as microalgae can generate strong long-lasting thrust for self-propulsion at a fast speed.

4. Biocompatibility

Biocompatibility is critical for designing microrobots for biomedical applications. In most cases, due to various requirements for drive, control, and functionality, the selected biotemplates cannot be used without toxicity. Therefore, in the design process, biotemplates should meet the minimum requirements for biocompatibility.

5. Living organisms' self-propulsion

Currently, most intelligent micro/nanorobots are based on inanimate biotemplates. However, biotemplates with life activity usually have unique characteristics or motion properties. Making full use of biotemplates with life activity and integrating the autonomous response, autonomous motion and self-healing properties to develop intelligent micro/nanorobots with dynamic response and autonomous adaptive working is very significant.



6. Multifunctional materials

Multifunctional materials are the future research trend, not only integrating materials but also combining multiple functions such as imaging, sensing, therapeutic and restorative environments in one system to achieve multifunctional applications.

Biotemplates not only have unique structures but also have specific functions, and are an important development direction in the future development of intelligent micro/nanorobots. We believe that with the development and the expansion of biotemplates and micro- and nanotechnology, the future intelligent micro/nanorobots will be more intelligent, efficient and safe, and become a brand new technological revolution to solve complex problems in the microscopic field in the future.

Note

There are no ethical concerns in this review.

Author contributions

T. Chen conceived the review and wrote the manuscript. Y. Cai, B. J. Sánchez, B. Ren, and R. Dong supervised the review and finalized the manuscript. All authors have given approval to the final version of the article.

Conflicts of interest

There are no conflicts to declare.

Acknowledgements

This work was supported by General Project of Natural Science Foundation of Guangdong Province (2022A1515010715) and Research and development plan projects in key areas of Guangdong Province (2020B0101030005). B. J. S acknowledges support from the Spanish Ministry of Science, Innovation and Universities [Grant PID2020-118154GB-I00 funded by MCIN/AEI/10.13039/501100011033, grant TED2021-132720B-I00, funded by MCIN/AEI/10.13039/501100011033 and the European Union "NextGenerationEU"/PRTR; grant CNS2023-144653] and the Universidad de Alcalá [Línea de Actuación Excelencia para el Profesorado Universitario de la UAH, EPU-INV-UAH/2022/003].

References

- 1 L. Wang, Y. Shi, J. Jiang, C. Li, H. Zhang, X. Zhang, T. Jiang, L. Wang, Y. Wang and L. Feng, *Small*, 2022, e2203678, DOI: [10.1002/sml.202203678](https://doi.org/10.1002/sml.202203678).
- 2 H. Wang and M. Pumera, *Adv. Funct. Mater.*, 2018, 28.
- 3 W. Liu, X. Chen, X. Lu, J. Wang, Y. Zhang and Z. Gu, *Adv. Funct. Mater.*, 2020, 30.
- 4 Q. Wang, R. Dong, Q. Yang, J. Wang, S. Xu and Y. Cai, *Nanoscale Horiz.*, 2020, 5, 325–330.
- 5 C. Wang, Q. Wang, R.-F. Dong and Y.-P. Cai, *Inorg. Chem. Commun.*, 2018, 91, 8–15.
- 6 D. Jin and L. Zhang, *Acc. Chem. Res.*, 2022, 55, 98–109.
- 7 P. L. Venugopalan, B. Esteban-Fernandez de Avila, M. Pal, A. Ghosh and J. Wang, *ACS Nano*, 2020, 14, 9423–9439.
- 8 J. Park, J. Y. Kim, S. Pane, B. J. Nelson and H. Choi, *Adv. Healthcare Mater.*, 2021, 10, e2001096.
- 9 B. Ezhilan, W. Gao, A. Pei, I. Rozen, R. Dong, B. Jurado-Sanchez, J. Wang and D. Saintillan, *Nanoscale*, 2015, 7, 7833–7840.
- 10 Q. Zhang, R. Dong, Y. Wu, W. Gao, Z. He and B. Ren, *ACS Appl. Mater. Interfaces*, 2017, 9, 4674–4683.
- 11 Z. Wu, T. Li, W. Gao, T. Xu, B. Jurado-Sánchez, J. Li, W. Gao, Q. He, L. Zhang and J. Wang, *Adv. Funct. Mater.*, 2015, 25, 3881–3887.
- 12 B. Esteban-Fernandez de Avila, A. Martin, F. Soto, M. A. Lopez-Ramirez, S. Campuzano, G. M. Vasquez-Machado, W. Gao, L. Zhang and J. Wang, *ACS Nano*, 2015, 9, 6756–6764.
- 13 M. Mathesh, J. Sun, F. van der Sandt and D. A. Wilson, *Nanoscale*, 2020, 12, 22495–22501.
- 14 W. Wang, Z. Wu, X. Lin, T. Si and Q. He, *J. Am. Chem. Soc.*, 2019, 141, 6601–6608.
- 15 J. Katuri, X. Ma, M. M. Stanton and S. Sanchez, *Acc. Chem. Res.*, 2017, 50, 2–11.
- 16 Y. Si, Z. Dong and L. Jiang, *ACS Cent. Sci.*, 2018, 4, 1102–1112.
- 17 W. Gao, X. Feng, A. Pei, C. R. Kane, R. Tam, C. Hennessy and J. Wang, *Nano Lett.*, 2014, 14, 305–310.
- 18 H. Zhou, T. Fan and D. Zhang, *ChemSusChem*, 2011, 4, 1344–1387.
- 19 D. Ni, L. Wang, Y. Sun, Z. Guan, S. Yang and K. Zhou, *Angew. Chem., Int. Ed.*, 2010, 49, 4223–4227.
- 20 Y. Pan, W. J. Paschoalino, A. Szuchmacher Blum and J. Mauzeroll, *ChemSusChem*, 2021, 14, 758–791.
- 21 J. Zhao, Y. Li, X. Chen, H. Zhang, C. Song, Z. Liu, K. Zhu, K. Cheng, K. Ye, J. Yan, D. Cao, G. Wang and X. Zhang, *Electrochim. Acta*, 2018, 292, 458–467.
- 22 Y. Xia, R. Fang, Z. Xiao, L. Ruan, R. Yan, H. Huang, C. Liang, Y. Gan, J. Zhang, X. Tao and W. Zhang, *RSC Adv.*, 2016, 6, 69764–69772.
- 23 Z. Lin, T. Jiang and J. Shang, *Bio-Des. Manuf.*, 2021, 5, 107–132.
- 24 Y. Alapan, O. Yasa, B. Yigit, I. C. Yasa, P. Erkoç and M. Sitti, *Ann. Rev. Control Robot. Auton. Syst.*, 2019, 2, 205–230.
- 25 N. Buss, O. Yasa, Y. Alapan, M. B. Akolpoglu and M. Sitti, *APL Bioeng.*, 2020, 4, 026103.
- 26 L. Bi and G. Pan, *J. Mater. Chem. A*, 2014, 2, 3715–3718.
- 27 A. Mahto, A. Singh, K. Aruchamy, A. Maraddi, G. R. Bhadu, N. S. Kotrappanavar and R. Meena, *Sustainable Mater. Technol.*, 2021, 29.
- 28 G. Huang, F. Chen, Y. Kuang, H. He and A. Qin, *Appl. Biochem. Biotechnol.*, 2016, 178, 1220–1238.
- 29 P. Rani and R. Srivastava, *Chem. Rec.*, 2020, 20, 968–988.
- 30 L. Lu, J. Li, J. Yu, P. Song and D. H. L. Ng, *Chem. Eng. J.*, 2016, 283, 524–534.



- 31 W. Li, Z. Chen, H. Yu, J. Li and S. Liu, *Adv. Mater.*, 2021, **33**, e2000596.
- 32 J. A. Gomez, K. Höffner and P. I. Barton, *Green Chem.*, 2016, **18**, 461–475.
- 33 O. I. Senturk, O. Schauer, F. Chen, V. Sourjik and S. V. Wegner, *Adv. Healthcare Mater.*, 2020, **9**, e1900956.
- 34 N. Pellicciotta, O. S. Bagal, V. C. Sosa, G. Frangipane, G. Vizsnyiczai and R. D. Leonardo, *Adv. Funct. Mater.*, 2023, **33**.
- 35 H. Li, L. Wang, Y. Wei, W. Yan and J. Feng, *Front. Chem.*, 2022, **10**, 882876.
- 36 F. Duan, Y. Zhu, H. Yu and A. Wang, *Colloids Surf., A*, 2022, **648**.
- 37 X. Li, F. Qu, W. Li, H. Lin and Y. Jin, *J. Sol-Gel Sci. Technol.*, 2012, **63**, 416–424.
- 38 V. R. Franceschi and P. A. Nakata, *Annu. Rev. Plant Biol.*, 2005, **56**, 41–71.
- 39 S. K. Srivastava, M. Medina-Sanchez, B. Koch and O. G. Schmidt, *Adv. Mater.*, 2016, **28**, 832–837.
- 40 L.-F. Chen, S.-X. Ma, S. Lu, Y. Feng, J. Zhang, S. Xin and S.-H. Yu, *Nano Res.*, 2016, **10**, 1–11.
- 41 T. Maric, M. Z. M. Nasir, N. F. Rosli, M. Budanović, R. D. Webster, N. J. Cho and M. Pumera, *Adv. Funct. Mater.*, 2020, **30**.
- 42 J. Liu, J. Li, G. Wang, W. Yang, J. Yang and Y. Liu, *J. Colloid Interface Sci.*, 2019, **555**, 234–244.
- 43 J. Liu, T. Xu, Y. Guan, X. Yan, C. Ye and X. Wu, *Micro-machines*, 2017, **8**.
- 44 H. Wang, M. G. Potroz, J. A. Jackman, B. Khezri, T. Marić, N.-J. Cho and M. Pumera, *Adv. Funct. Mater.*, 2017, **27**.
- 45 N. Ebrahimi, C. Bi, D. J. Cappelleri, G. Ciuti, A. T. Conn, D. Faivre, N. Habibi, A. Hošovský, V. Iacovacci, I. S. M. Khalil, V. Magdanz, S. Misra, C. Pawashe, R. Rashidifar, P. E. D. Soto-Rodriguez, Z. Fekete and A. Jafari, *Adv. Funct. Mater.*, 2020, **31**.
- 46 Z. H. Wang, A. Klingner, V. Magdanz, S. Misra and I. S. M. Khalil, *Adv. Intell. Syst.*, 2023, **6**.
- 47 C. H. Villa, A. C. Anselmo, S. Mitragotri and V. Muzykantov, *Adv. Drug Delivery Rev.*, 2016, **106**, 88–103.
- 48 L. Sun, Y. Yu, Z. Chen, F. Bian, F. Ye, L. Sun and Y. Zhao, *Chem. Soc. Rev.*, 2020, **49**, 4043–4069.
- 49 W. Wang and S. Wang, *Lab Chip*, 2022, **22**, 1042–1067.
- 50 T. Liu, C. Gao, D. Gu and H. Tang, *Drug Delivery Transl. Res.*, 2022, **12**, 2634–2648.
- 51 J. Wang, R. Ahmed, Y. Zeng, K. Fu, F. Soto, B. Sinclair, H. T. Soh and U. Demirci, *Small*, 2020, **16**, e2005185.
- 52 Z. Wu, T. Li, J. Li, W. Gao, T. Xu, C. Christianson, W. Gao, M. Galarnyk, Q. He, L. Zhang and J. Wang, *ACS Nano*, 2014, **8**, 12041–12048.
- 53 J. S. Brenner, D. C. Pan, J. W. Myerson, O. A. Marcos-Contreras, C. H. Villa, P. Patel, H. Hekierski, S. Chatterjee, J. Q. Tao, H. Parhiz, K. Bhamidipati, T. G. Uhler, E. D. Hood, R. Y. Kiseleva, V. S. Shuvaev, T. Shuvaeva, M. Khoshnejad, I. Johnston, J. V. Gregory, J. Lahann, T. Wang, E. Cantu, W. M. Armstead, S. Mitragotri and V. Muzykantov, *Nat. Commun.*, 2018, **9**, 2684.
- 54 X. Pan, Q. Wang, S. Li, X. Wang and X. Han, *ChemistrySelect*, 2019, **4**, 10296–10298.
- 55 Q. Chen, S. Tang, Y. Li, Z. Cong, D. Lu, Q. Yang, X. Zhang and S. Wu, *ACS Appl. Mater. Interfaces*, 2021, **13**, 58382–58392.
- 56 C. Caroppo and P. Pagliara, *Microorganisms*, 2022, **10**.
- 57 F. G. A. Fernandez, A. Reis, R. H. Wijffels, M. Barbosa, V. Verdelho and B. Llamas, *New Biotechnol.*, 2021, **61**, 99–107.
- 58 S. Gomez-Zorita, J. Trepiana, M. Gonzalez-Arceo, L. Aguirre, I. Milton-Laskibar, M. Gonzalez, I. Eseberri, A. Fernandez-Quintela and M. P. Portillo, *Int. J. Mol. Sci.*, 2019, **21**.
- 59 L. Tounsi, F. Hentati, H. Ben Hlima, M. Barkallah, S. Smaoui, I. Fendri, P. Michaud and S. Abdelkafi, *Int. J. Biol. Macromol.*, 2022, **221**, 1238–1250.
- 60 K. A. Martinez Andrade, C. Lauritano, G. Romano and A. Ianora, *Mar. Drugs*, 2018, **16**.
- 61 Z. C. Liang, M. H. Liang and J. G. Jiang, *Crit. Rev. Food Sci. Nutr.*, 2020, **60**, 3195–3213.
- 62 F. Zhang, Z. Li, C. Chen, H. Luan, R. H. Fang, L. Zhang and J. Wang, *Adv. Mater.*, 2024, **36**, e2303714.
- 63 E. S. J. Thore, K. Muylaert, M. G. Bertram and T. Brodin, *Curr. Biol.*, 2023, **33**, R91–R95.
- 64 X. Yan, J. Xu, Q. Zhou, D. Jin, C. I. Vong, Q. Feng, D. H. L. Ng, L. Bian and L. Zhang, *Appl. Mater. Today*, 2019, **15**, 242–251.
- 65 H. Xin, N. Zhao, Y. Wang, X. Zhao, T. Pan, Y. Shi and B. Li, *Nano Lett.*, 2020, **20**, 7177–7185.
- 66 J. Xiong, Y. Shi, T. Pan, D. Lu, Z. He, D. Wang, X. Li, G. Zhu, B. Li and H. Xin, *Adv. Sci.*, 2023, **10**, e2301365.
- 67 L. Liu, J. Wu, B. Chen, J. Gao, T. Li, Y. Ye, H. Tian, S. Wang, F. Wang, J. Jiang, J. Ou, F. Tong, F. Peng and Y. Tu, *ACS Nano*, 2022, **16**, 6515.
- 68 A. Panda, A. S. Reddy, S. Venkateswarlu and M. Yoon, *Nanoscale*, 2018, **10**, 16268–16277.
- 69 O. Yasa, P. Erkoc, Y. Alapan and M. Sitti, *Adv. Mater.*, 2018, **30**, e1804130.
- 70 X. Wang, J. Cai, L. Sun, S. Zhang Gong, X. Li, S. Yue, L. Feng and D. Zhang, *ACS Appl. Mater. Interfaces*, 2019, **11**, 4745–4756.
- 71 H. W. Shim, A. H. Lim, J. C. Kim, E. Jang, S. D. Seo, G. H. Lee, T. D. Kim and D. W. Kim, *Sci. Rep.*, 2013, **3**, 2325.
- 72 Y. Liu, C. Zhu, F. Wan, W. Fang, B. Xue, Z. Zheng, H. Ping, H. Xie, H. Wang, W. Wang and Z. Fu, *Giant*, 2022, **11**.
- 73 U. Goswami, A. K. Sahoo, A. Chattopadhyay and S. S. Ghosh, *ACS Omega*, 2018, **3**, 6113–6119.
- 74 E. B. Steager, M. S. Sakar, D. H. Kim, V. Kumar, G. J. Pappas and M. J. Kim, *J. Micromech. Microeng.*, 2011, **21**.
- 75 T. Gwisai, N. Mirkhani, M. G. Christiansen, T. T. Nguyen, V. Ling and S. Schuerle, *Sci. Robot.*, 2022, **7**, eabo0665.
- 76 S. J. Park, S. H. Park, S. Cho, D. M. Kim, Y. Lee, S. Y. Ko, Y. Hong, H. E. Choy, J. J. Min, J. O. Park and S. Park, *Sci. Rep.*, 2013, **3**, 3394.
- 77 H. Chen, Y. Li, Y. Wang, P. Ning, Y. Shen, X. Wei, Q. Feng, Y. Liu, Z. Li, C. Xu, S. Huang, C. Deng, P. Wang and Y. Cheng, *ACS Nano*, 2022, **16**, 6118–6133.



- 78 J. Xing, T. Yin, S. Li, T. Xu, A. Ma, Z. Chen, Y. Luo, Z. Lai, Y. Lv, H. Pan, R. Liang, X. Wu, M. Zheng and L. Cai, *Adv. Funct. Mater.*, 2020, 31.
- 79 D. Yang, T. Fan, D. Zhang, J. Zhu, Y. Wang, B. Du and Y. Yan, *Chemistry*, 2013, **19**, 4742–4747.
- 80 Y. Sun and Z. Guo, *Nanoscale Horiz.*, 2019, **4**, 52–76.
- 81 J. Liu, K. Zhang, H. Wang, L. Lin, J. Zhang, P. Li, Q. Zhang, J. Shi and H. Cui, *Polymers*, 2022, 14.
- 82 D. Liu, T. Zhang, Y. Guo, Y. Liao, Z. Wu, H. Jiang and Y. Lu, *ACS Appl. Bio Mater.*, 2022, **5**, 5933–5942.
- 83 W. Yang, J. Li, Z. Xu, J. Yang, Y. Liu and L. Liu, *J. Mater. Chem. C*, 2019, **7**, 10297–10308.
- 84 S. Tottori, L. Zhang, F. Qiu, K. K. Krawczyk, A. Franco-Obregon and B. J. Nelson, *Adv. Mater.*, 2012, **24**, 811–816.
- 85 M. Zhou, Y. Xing, X. Li, X. Du, T. Xu and X. Zhang, *Small*, 2020, **16**, e2003834.
- 86 J. Zhao, Q. Shao, S. Ge, J. Zhang, J. Lin, D. Cao, S. Wu, M. Dong and Z. Guo, *Chem. Rec.*, 2020, **20**, 710–729.
- 87 T. Chen, H. Zhao, Y. Zheng, Y. Cai, B. Ren and R. Dong, *Chem. Eng. J.*, 2022, 439.
- 88 S.-J. Song, C. C. Mayorga-Martinez, D. Huska and M. Pumera, *NPG Asia Mater.*, 2022, 14.
- 89 D. Huska, C. C. Mayorga-Martinez, R. Zelinka and M. Pumera, *Small*, 2022, **18**, e2200208.
- 90 Y. Han, Y. Lyu, N. Xing, X. Zhang, K. Hu, H. Luo, D. H. L. Ng and J. Li, *J. Mater. Chem. C*, 2022, **10**, 15524–15531.
- 91 J. Li, F. Ji, D. H. L. Ng, J. Liu, X. Bing and P. Wang, *Chem. Eng. J.*, 2019, **369**, 611–620.
- 92 M. Sun, X. Fan, X. Meng, J. Song, W. Chen, L. Sun and H. Xie, *Nanoscale*, 2019, **11**, 18382–18392.
- 93 M. Sun, K. F. Chan, Z. Zhang, L. Wang, Q. Wang, S. Yang, S. M. Chan, P. W. Y. Chiu, J. J. Y. Sung and L. Zhang, *Adv. Mater.*, 2022, **34**, e2201888.
- 94 L. Song, J. Cai, S. Zhang, B. Liu, Y.-D. Zhao and W. Chen, *Sens. Actuators, B*, 2022, 358.
- 95 L. B. Song, S. J. Zhang, Q. M. Wang, W. Chen, B. Liu and Y. D. Zhao, *Chem. Eng. J.*, 2022, 435.
- 96 C. C. Mayorga-Martinez, M. Fojtů, J. Vyskočil, N. J. Cho and M. Pumera, *Adv. Funct. Mater.*, 2022, **32**(46), 2207272.
- 97 M. Sun, W. Chen, X. Fan, C. Tian, L. Sun and H. Xie, *Appl. Mater. Today*, 2020, 20.
- 98 M. Sun, Q. Liu, X. Fan, Y. Wang, W. Chen, C. Tian, L. Sun and H. Xie, *Small*, 2020, **16**, e1906701.
- 99 Q. Wang, S. Jermyn, D. Quashie, Jr., S. E. Gatti, J. Katuri and J. Ali, *RSC Adv.*, 2023, **13**, 30951–30958.
- 100 V. Magdanz, I. S. M. Khalil, J. Simmchen, G. P. Furtado, S. Mohanty, J. Gebauer, H. Xu, A. Klingner, A. Aziz, M. Medina-Sanchez, O. G. Schmidt and S. Misra, *Sci. Adv.*, 2020, **6**, eaba5855.
- 101 K. Middelhoek, V. Magdanz, L. Abelman and I. S. M. Khalil, *Biomed. Mater.*, 2022, 17.
- 102 F. Striggow, C. Ribeiro, A. Aziz, R. Nauber, F. Hebenstreit, O. G. Schmidt and M. Medina-Sanchez, *Small*, 2023, e2310288, DOI: [10.1002/smll.202310288](https://doi.org/10.1002/smll.202310288).
- 103 H. Xu, M. Medina-Sanchez, W. Zhang, M. P. H. Seaton, D. R. Brison, R. J. Edmondson, S. S. Taylor, L. Nelson, K. Zeng, S. Bagley, C. Ribeiro, L. P. Restrepo, E. Lucena, C. K. Schmidt and O. G. Schmidt, *Nanoscale*, 2020, **12**, 20467–20481.
- 104 C. Chen, X. Chang, P. Angsantikul, J. Li, B. Esteban-Fernández de Ávila, E. Karshalev, W. Liu, F. Mou, S. He, R. Castillo, Y. Liang, J. Guan, L. Zhang and J. Wang, *Adv. Biosyst.*, 2017, 2.
- 105 C. C. Mayorga-Martinez, J. Zelenka, J. Grmela, H. Michalkova, T. Ruml, J. Mares and M. Pumera, *Adv. Sci.*, 2021, **8**, e2101301.
- 106 L. Xu, D. Gong, N. Celi, J. Xu, D. Zhang and J. Cai, *Appl. Surf. Sci.*, 2022, 579.
- 107 D. Gong, Y. Li, H. Zhou, B. Gu, N. Celi, D. Zhang and J. Cai, *Appl. Mater. Today*, 2023, 35.
- 108 B. Gu, J. Cai, G. Peng, H. Zhou, W. Zhang, D. Zhang and D. Gong, *Colloids Surf., A*, 2024, 685.
- 109 De Gong, N. Celi, D. Zhang and J. Cai, *ACS Appl. Mater. Interfaces*, 2022, **14**, 6320–6330.
- 110 X. Peng, M. Urso, M. Kolackova, D. Huska and M. Pumera, *Adv. Funct. Mater.*, 2024, 34.
- 111 De Gong, B. Li, N. Celi, J. Cai and D. Zhang, *ACS Appl. Mater. Interfaces*, 2021, **13**(44), 53131–53142.
- 112 D. Gong, N. Celi, L. Xu, D. Zhang and J. Cai, *Mater. Today Chem.*, 2022, 23.
- 113 L. Xie, X. Pang, X. Yan, Q. Dai, H. Lin, J. Ye, Y. Cheng, Q. Zhao, X. Ma, X. Zhang, G. Liu and X. Chen, *ACS Nano*, 2020, **14**, 2880–2893.
- 114 C. Zheng, Z. Li, T. Xu, L. Chen, F. Fang, D. Wang, P. Dai, Q. Wang, X. Wu and X. Yan, *Appl. Mater. Today*, 2021, 22.
- 115 A. Terzopoulou, M. Palacios-Corella, C. Franco, S. Sevim, T. Dysli, F. Mushtaq, M. Romero-Angel, C. Marti-Gastaldo, D. Gong, J. Cai, X. Z. Chen, M. Pumera, A. J. DeMello, B. J. Nelson, S. Pané and J. Puigmartí-Luis, *Adv. Funct. Mater.*, 2021, 32.
- 116 V. de la Asuncion-Nadal, C. Franco, A. Veciana, S. Ning, A. Terzopoulou, S. Sevim, X. Z. Chen Gong, J. Cai, P. D. Wendel-Garcia, B. Jurado-Sanchez, A. Escarpa, J. Puigmartí-Luis and S. Pane, *Small*, 2022, e2203821, DOI: [10.1002/smll.202203821](https://doi.org/10.1002/smll.202203821).
- 117 L. Liu, J. Wu, S. Wang, L. Kun, J. Gao, B. Chen, Y. Ye, F. Wang, F. Tong, J. Jiang, J. Ou, D. A. Wilson, Y. Tu and F. Peng, *Nano Lett.*, 2021, **21**, 3518–3526.
- 118 D. Zhong, W. Li, Y. Qi, J. He and M. Zhou, *Adv. Funct. Mater.*, 2020, 30.
- 119 X. Yan, Q. Zhou, M. Vincent, Y. Deng, J. Yu, J. Xu, T. Xu, T. Tang, L. Bian, Y. J. Wang, K. Kostarelos and L. Zhang, *Sci. Robot.*, 2017, 2.
- 120 F. Zhang, Z. Li, Y. Duan, H. Luan, L. Yin, Z. Guo, C. Chen, M. Xu, W. Gao, R. H. Fang, L. Zhang and J. Wang, *Sci. Adv.*, 2022, **8**, eade6455.
- 121 F. Zhang, J. Zhuang, Z. Li, H. Gong, B. E. de Avila, Y. Duan, Q. Zhang, J. Zhou, L. Yin, E. Karshalev, W. Gao, V. Nizet, R. H. Fang, L. Zhang and J. Wang, *Nat. Mater.*, 2022, **21**, 1324–1332.
- 122 I. S. Shchelikh, J. V. D. Molino and K. Gademann, *Acta Biomater.*, 2021, **136**, 99–110.



- 123 M. B. Akolpoglu, N. O. Dogan, U. Bozuyuk, H. Ceylan, S. Kizilel and M. Sitti, *Adv. Sci.*, 2020, **7**, 2001256.
- 124 T. Pan, Y. Shi, N. Zhao, J. Xiong, Y. Xiao, H. Xin and B. Li, *Adv. Funct. Mater.*, 2021, **32**.
- 125 X. J. Teng, W. M. Ng, W. H. Chong, D. J. C. Chan, R. Mohamud, B. S. Ooi, C. Guo, C. Z. Liu and J. Lim, *Langmuir*, 2021, **37**, 9192–9201.
- 126 H. Choi, B. Kim, S. H. Jeong, T. Y. Kim, D. P. Kim, Y. K. Oh and S. K. Hahn, *Small*, 2023, **19**, e2204617.
- 127 T. Studer, D. Morina, I. S. Shchelikh and K. Gademann, *Chemistry*, 2023, **29**, e202203913.
- 128 F. Zhang, Z. Li, L. Yin, Q. Zhang, N. Askarinam, R. Mundaca-Urbe, F. Tehrani, E. Karshalev, W. Gao, L. Zhang and J. Wang, *J. Am. Chem. Soc.*, 2021, **143**, 12194–12201.
- 129 J. Xiong, X. Li, Z. He, Y. Shi, T. Pan, G. Zhu, D. Lu and H. Xin, *Light: Sci. Appl.*, 2024, **13**, 55.
- 130 M. Li, J. Wu, D. Lin, J. Yang, N. Jiao, Y. Wang and L. Liu, *Acta Biomater.*, 2022, **154**, 443–453.
- 131 J. Wang, F. Soto, S. Q. Liu, Q. Q. Yin, E. Purcell, Y. T. Zeng, E. C. Hsu, D. Akin, B. Sinclair, T. Stoyanova and U. Demirci, *Adv. Funct. Mater.*, 2022, **32**.
- 132 Y. Li, S. Tang, Z. Cong, D. Lu, Q. Yang, Q. Chen, X. Zhang and S. Wu, *Mater. Today Chem.*, 2022, **23**.
- 133 A. V. Singh, Z. Hosseinidoust, B. W. Park, O. Yasa and M. Sitti, *ACS Nano*, 2017, **11**, 9759–9769.
- 134 B. Mostaghaci, O. Yasa, J. Zhuang and M. Sitti, *Adv. Sci.*, 2017, **4**, 1700058.
- 135 M. B. Akolpoglu, Y. Alapan, N. O. Dogan, S. F. Baltaci, O. Yasa, G. Aybar Tural and M. Sitti, *Sci. Adv.*, 2022, **8**, eabo6163.
- 136 B. W. Park, J. Zhuang, O. Yasa and M. Sitti, *ACS Nano*, 2017, **11**, 8910–8923.
- 137 Z. Sun, P. F. Popp, C. Loderer and A. Revilla-Guarinos, *Sensors*, 2019, **20**.
- 138 J. Zhuang, R. Wright Carlsen and M. Sitti, *Sci. Rep.*, 2015, **5**, 11403.
- 139 Y. Zhang, L. Zhang, L. Yang, C. I. Vong, K. F. Chan, W. K. K. Wu, T. N. Y. Kwong, N. W. S. Lo, M. Ip, S. H. Wong, J. J. Y. Sung, P. W. Y. Chiu and L. Zhang, *Sci. Adv.*, 2019, **5**.
- 140 L. Yang, Y. Zhang, Q. Wang, K.-F. Chan and L. Zhang, *IEEE Trans. Auto. Sci. Eng.*, 2020, **17**, 490–501.
- 141 Y. Zhang, K. Yan, F. Ji and L. Zhang, *Adv. Funct. Mater.*, 2018, **28**.
- 142 X. Wei, M. Beltran-Gastelum, E. Karshalev, B. Esteban-Fernandez de Avila, J. Zhou, D. Ran, P. Angsantikul, R. H. Fang, J. Wang and L. Zhang, *Nano Lett.*, 2019, **19**, 1914–1921.
- 143 E. Karshalev, B. Esteban-Fernandez de Avila, M. Beltran-Gastelum, P. Angsantikul, S. Tang, R. Mundaca-Urbe, F. Zhang, J. Zhao, L. Zhang and J. Wang, *ACS Nano*, 2018, **12**, 8397–8405.
- 144 J. Wang, R. Dong, H. Wu, Y. Cai and B. Ren, *Nanomicro Lett.*, 2019, **12**, 11.
- 145 S. Wang, W. X. Ren, J. T. Hou, M. Won, J. An, X. Chen, J. Shu and J. S. Kim, *Chem. Soc. Rev.*, 2021, **50**, 8887–8902.
- 146 C. H. Park, H. Yun, H. Yang, J. Lee and B. J. Kim, *Adv. Funct. Mater.*, 2017, **27**.
- 147 T. L. Lefebvre, E. Brown, L. Hacker, T. Else, M. E. Oraiopoulou, M. R. Tomaszewski, R. Jena and S. E. Bohndiek, *Front. Oncol.*, 2022, **12**, 803777.
- 148 A. Khalil, M. Majlath, V. Gounant, A. Hess, J. P. Laissy and M. P. Debray, *Diagn. Interv. Imaging*, 2016, **97**, 991–1002.
- 149 M. Chen, L. Sun, Z. Hong, H. Wang, Y. Xia, S. Liu, X. Ren, X. Zhang, D. Chi, H. Yang and W. Hu, *ACS Appl. Mater. Interfaces*, 2022, **14**, 41275–41282.
- 150 C. Jin, X. Luo, X. Li, R. Zhou, Y. Zhong, Z. Xu, C. Cui, X. Xing, H. Zhang and M. Tian, *Cancer*, 2022, **128**, 2704–2716.
- 151 C. Gao, Y. Wang, Z. Ye, Z. Lin, X. Ma and Q. He, *Adv. Mater.*, 2021, **33**, e2000512.
- 152 A. Aziz, J. Holthof, S. Meyer, O. G. Schmidt and M. Medina-Sanchez, *Adv. Healthcare Mater.*, 2021, **10**, e2101077.
- 153 B. Wang, K. F. Chan, K. Yuan, Q. Wang, X. Xia, L. Yang, H. Ko, Y. J. Wang, J. J. Y. Sung, P. W. Y. Chiu and L. Zhang, *Sci. Robot.*, 2021, **6**.
- 154 M. B. Kulkarni, N. H. Ayachit and T. M. Aminabhavi, *Biosensors*, 2022, **12**.
- 155 H. Li, F. Peng, X. Yan, C. Mao, X. Ma, D. A. Wilson, Q. He and Y. Tu, *Acta Pharm. Sin. B*, 2022, **13**(2), 517–541.
- 156 X. Liu, J. Huang, Y. Li, Y. Zhang and B. Li, *Nanophotonics*, 2017, **6**, 309–316.
- 157 Y. Li, X. Liu, X. Xu, H. Xin, Y. Zhang and B. Li, *Adv. Funct. Mater.*, 2019, **29**.
- 158 Q. Xin, H. Shah, A. Nawaz, W. Xie, M. Z. Akram, A. Batool, L. Tian, S. U. Jan, R. Boddula, B. Guo, Q. Liu and J. R. Gong, *Adv. Mater.*, 2019, **31**, e1804838.
- 159 E. Ren, C. Zhang, D. Li, X. Pang and G. Liu, *View*, 2020, **1**.
- 160 F. Soto, M. A. Lopez-Ramirez, I. Jeerapan, B. Esteban-Fernandez de Avila, R. K. Mishra, X. Lu, I. Chai, C. Chen, D. Kupor, A. Nourhani and J. Wang, *Adv. Funct. Mater.*, 2019, **29**.
- 161 G. Volpe, I. Buttinoni, D. Vogt, H.-J. Kümmerer and C. Bechinger, *Soft Matter*, 2011, **7**.
- 162 C. Yang, Z. Chen, M. Wei, S. Hu, M. Cai, N. Wang, Y. Guan, F. Li, Q. Ding and D. Ling, *J. Controlled Release*, 2023, **357**, 20–30.
- 163 H. Xu, M. Medina-Sanchez, V. Magdanz, L. Schwarz, F. Hebenstreit and O. G. Schmidt, *ACS Nano*, 2018, **12**, 327–337.
- 164 F. Zhang, J. Zhuang, Z. Li, H. Gong, B. E. de Avila, Y. Duan, Q. Zhang, J. Zhou, L. Yin, E. Karshalev, W. Gao, V. Nizet, R. H. Fang, L. Zhang and J. Wang, *Nat. Mater.*, 2022, **21**, 1324–1332.
- 165 Y. Hu, W. Liu and Y. Sun, *Adv. Funct. Mater.*, 2022, **32**(10), 2109181.
- 166 E. Karshalev, B. Esteban-Fernandez de Avila and J. Wang, *J. Am. Chem. Soc.*, 2018, **140**, 3810–3820.
- 167 F. Mushtaq, X. Chen, S. Stauffert, H. Torlakcik, X. Wang, M. Hoop, A. Gerber, X. Li, J. Cai, B. J. Nelson and S. Pané, *J. Mater. Chem. A*, 2019, **7**, 24847–24856.
- 168 M. Jaishankar, T. Tseten, N. Anbalagan, B. B. Mathew and K. N. Beeregowda, *Interdiscip. Toxicol.*, 2014, **7**, 60–72.



- 169 V. K. Gupta, A. Nayak and S. Agarwal, *Environ. Eng. Res.*, 2015, **20**, 1–18.
- 170 B. Saha and C. Orvig, *Coord. Chem. Rev.*, 2010, **254**, 2959–2972.
- 171 C.-y Wang, K. Jiao, J.-f Yan, M.-c Wan, Q.-q Wan, L. Breschi, J.-h Chen, F. R. Tay and L.-n Niu, *Prog. Mater. Sci.*, 2021, 116.
- 172 Y. Liu, P. Wang, B. Gojenko, J. Yu, L. Wei, D. Luo and T. Xiao, *Environ. Pollut.*, 2021, **291**, 118209.
- 173 R. W. Chia, J.-Y. Lee, H. Kim and J. Jang, *Environ. Chem. Lett.*, 2021, **19**, 4211–4224.
- 174 E. M. John and J. M. Shaik, *Environ. Chem. Lett.*, 2015, **13**, 269–291.
- 175 D. Xu and H. Ma, *J. Cleaner Prod.*, 2021, 313.
- 176 N. Yousefi, X. Lu, M. Elimelech and N. Tufenkji, *Nat. Nanotechnol.*, 2019, **14**, 107–119.

